TECHNICAL REPORT LWL-CR-06P73

LINE INTRUSION DETECTOR

by

E. K. Stodola
Syracuse University Research Corporation
Merrill Lane, University Heights
Syracuse, New York 13210

May 1974

Final Report

Contract No. DAAD05-73-C-0782

APPROVED FOR PUBLIC RELEASE; DISTRIBUTION UNLIMITED

U. S. ARMY LAND WARFARE LABORATORY
Aberdeen Proving Ground, Maryland 21005

The findings in this report are not to be construed as an official Department of the Army position unless so designated by other authorized documents.

REPORT DOCUMENTATION PAGE

READ INSTRUCTIONS BEFORE COMPLETING FORM

1. REPORT NUMBER: LWL-CR-06P73	2. GOVT ACCESSION NO.
3. RECIPIENT'S CATALOG NUMBER	
4. TITLE (and Subtitle): Line Intrusion Detector	5. TYPE OF REPORT & PERIOD COVERED: Final Report
6. PERFORMING ORG. REPORT NUMBER: SURC TR-74-107	
7. AUTHOR(s): E. K. Stodola	8. CONTRACT OR GRANT NUMBER(s): DAAD05-73-C-0782
9. PERFORMING ORGANIZATION NAME AND ADDRESS: Syracuse University Research Corporation, Merrill Lane, University Heights, Syracuse, New York 13210	10. PROGRAM ELEMENT, PROJECT, TASK AREA & WORK UNIT NUMBERS: 06-P-73
11. CONTROLLING OFFICE NAME AND ADDRESS: US Army Land Warfare Laboratory, Aberdeen Proving Ground, MD 21005	12. REPORT DATE: May 1974 13. NUMBER OF PAGES: 56
14. MONITORING AGENCY NAME & ADDRESS (if different from Controlling Office)	15. SECURITY CLASS. (of this report): Unclassified 15a. DECLASSIFICATION/DOWNGRADING SCHEDULE

16. DISTRIBUTION STATEMENT (of this Report)

Approved for public release; distribution unlimited

17. DISTRIBUTION STATEMENT (of the abstract entered in Block 20, if different from Report)

18. SUPPLEMENTARY NOTES

19. KEY WORDS (Continue on reverse side if necessary and identify by block number)

Intrusion detector
Radiating line antennas
Goubau line
RADIAX cable
Radar intrusion detector

20. ABSTRACT (Continue on reverse side if necessary and identify by block number)

Several radiating line configurations were experimentally evaluated for use in a line-type intrusion detection system. The types of radiating lines examined were Radiax cable, Goubau line and television twin lead (300 ohm). Measurements of dissipative and radiation losses were made at 140 and 915 MH_z and these data are presented, together with theoretical considerations related to a line intrusion detection system.

DD FORM 1 JAN 73 1473 EDITION OF 1 NOV 65 IS OBSOLETE

AD-780719

TABLE OF CONTENTS

	Page
REPORT DOCUMENTATION PAGE (DD FORM 1473)	iii
FOREWORD	v
LIST OF ILLUSTRATIONS	vi
LIST OF TABLES	vii
1. GENERAL	1
2. ANALYTIC MODEL	1
3. LINES TESTED	4
4. TEST ARRANGEMENT	9
5. TEST RESULTS	16
6. CONCLUSIONS	24
7. RECOMMENDATIONS	24
8. DELIVERED ITEMS	25
APPENDIX	
A. DERIVATION OF RANGE EQUATIONS FOR LINE INTRUSION DETECTOR AND LINE DESIGN OPTIMIZATION	26
DISTRIBUTION LIST	53

FOREWARD

This effort was sponsored by the US Army Land Warfare Laboratory, Advanced Development Division, Applied Physics Branch under the technical supervision of Mr. H. T. Lootens. The project was titled Line Intrusion Detector, LWL Task No. 06-P-73.

As a result of the disestablishment of the Land Warfare Laboratory on 30 June 1974, this project was transferred to the Counter Mine/ Counter Intrusion Division, MERDC, Ft. Belvoir, VA. Point of contact there is Mr. Robert Brubaker, Autovon 354-6941/4644.

LIST OF ILLUSTRATIONS

Figure		Page
1	Bistatic Line Intrusion Radar	2
2	Conceptual Model of Bistatic Intrusion Radar	5
3	An Overall Radar Equation for "Bistatic" Radar	6
4	Discontinuities Introduced in Goubau Line to Increase Radiation	10
5	Unmodified Twin Lead and Discontinuities Added to Increase Radiation	11
6	Moving Target Simulator for Test of Intrusion Line Radar	13
7	Simulation of a Long Line by Use of a Short Section and Auxiliary Attenuation	14
8	Block Diagram of Signal Measurement System Using ARI Radar Transmitter and Receiver (Processing and Alarm Elements Not Used)	15
9	Lines and Line Perturbation Methods	17
10	Sensitivity Measure as a Function of Line Radiation in a Bistatic Line Intrusion Detector	19
11	Plot of Actual and Predicted Results	22

LIST OF TABLES

Table		Page
1	Objectives of Contract DAAD05-73-C-0782	3
2	Determination of Optimum Line Radiation	7
3	Summary of Dissipative and Radiation Losses of Lines	18
4	Predicted Test Results with Oscillating Target	20

1. GENERAL

The contract was directed to an investigation of possible radiating line configurations for a line type intrusion detection radar and, in addition, required the provision of several deliverable lines to be based upon the results of that investigation. The type of radar device visualized for use with the line is illustrated in Figure 1. In this illustration the line connecting the transmitter and receiver is relatively long, and the target couples with the line at a relatively short region along the line in the general vicinity of the target.

The specific contract objectives are presented in summary form in Table 1. The summary takes account of the various amendments to the contract which occurred during its progress.

2. ANALYTIC MODEL

An analytic model for the behavior of the line type radar was developed as part of the contract performance, and the development of this model and some of the associated matter is given in full in SURC TN-73-373 entitled "DERIVATION OF RANGE EQUATIONS FOR LINE INTRUSION DETECTOR AND LINE DESIGN OPTIMIZATION," which is included as Appendix A to this report.

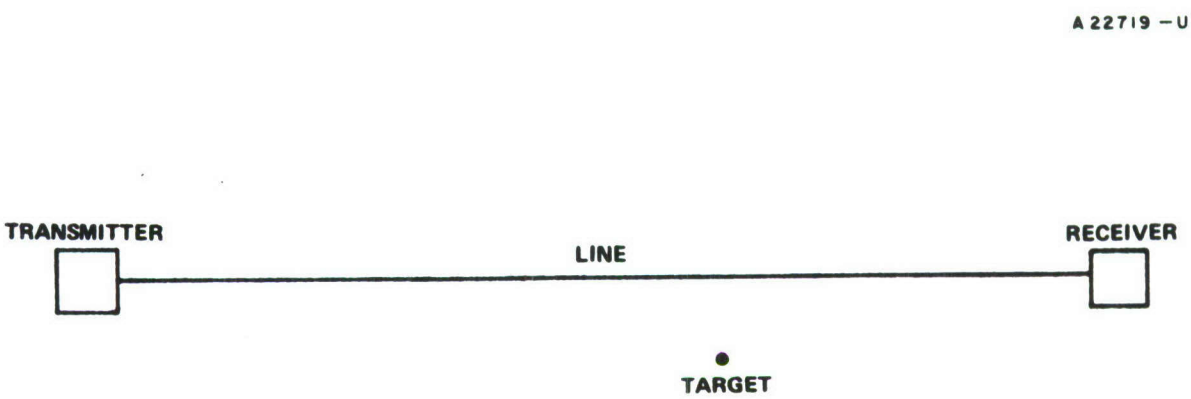

Figure 1 Bistatic Line Intrusion Radar

TABLE 1

Objectives of Contract
DAAD05-73-C-0782

1. FOR INTRUSION DETECTION RADAR LINE TYPE ANTENNA:

   - EVALUATE LINE DISSIPATIVE AND RADIATION LOSS
   - EVALUATE RECEIVED SIGNAL LEVEL AS A FUNCTION OF DISTANCE OF THE TARGET FROM THE LINE
   - RELATE THESE DATA TO SYSTEM ANALYTIC MODEL

   THE ABOVE EXPERIMENTS TO BE PERFORMED FOR:

   - RADIAX CABLE AT 140 AND 915 MHz
   - GOUBAU LINE WITH AND WITHOUT DISCONTINUITIES AT 915 MHz
   - 300 Ω TWIN LEAD LINE WITH AND WITHOUT DISCONTINUITIES AT 915 MHz

2. DELIVERABLE ITEMS BASED ON THE DATA DEVELOPED ABOVE ARE:

   - 1000 ft WIRE FOR GOUBAU LINE WITH PERTURBERS WHICH CAN BE INSERTED TO SYSTEMATICALLY INTRODUCE DISCONTINUITIES IN THE LINE, AND COAXIAL LINE CONNECTOR COUPLING HORNS FOR EACH END OF THE LINE
   - A 300 Ω TWIN LEAD LINE TRANSMISSION LINE OF LENGTH BASED ON RESULTS OF EXPERIMENTS, AND WITH PERTURBERS TO SYSTEMATICALLY INTRODUCE DISCONTINUITIES IN THE LINE

The conceptual model upon which the derivation is based and some of the definitions related thereto are given in Figure 2. The radar equation which was developed in this analysis and some of its ramifications are given in Figure 3. This figure summarizes the analysis which is given in the Appendix.

An important conclusion from the equations developed is the determination of the optimum radiation factor which the line should possess to provide maximum target sensitivity. This conclusion and its background are summarized in Table 2.

It is shown in Table 2 that the optimum radiation factor for the line is 8.69 dB regardless of the length of the line. This is to say that, although the sensitivity is reduced by increasing the length of the line, for any selected line the radiation from the line should constitute 8.69 dB of the total loss in the line. This figure involves only the radiative factor, and to it must be added the line dissipative loss if the total attenuation from one end of the line to the other is to be determined. Clearly, the greater the purely dissipative loss the lower will be the sensitivity of the radar system.

3. LINES TESTED

As indicated in Table 1 three types of lines were to be investigated, namely:

1. Radiax cable, a commercially available line with radiative qualities intentionally included with its transmission quality. Early experiments with this line indicated completely unsatisfactory radar operation. Useful measurement at both 140 and at 915 MHz frequencies were found impossible, and attempts to use the Radiax cable were abandoned.

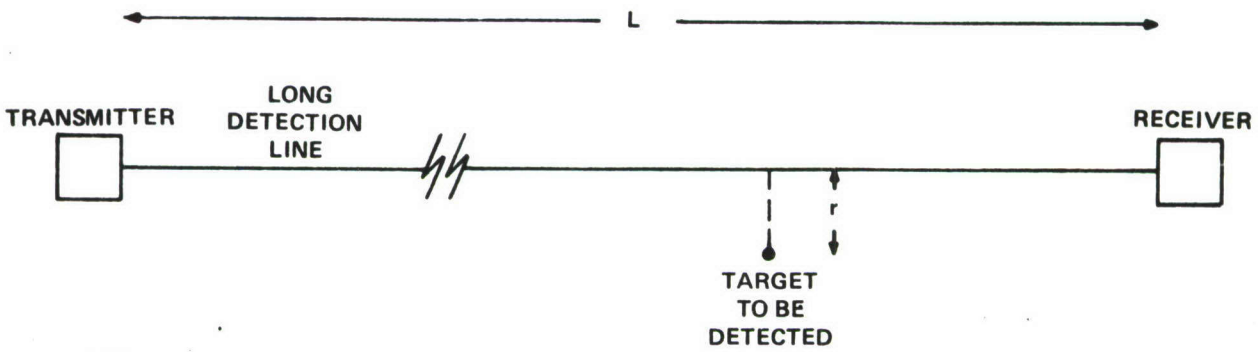

ASSUMPTIONS:

- TARGET COUPLES BETWEEN TRANSMITTER AND RECEIVER ONLY BECAUSE OF LINE RADIATION IN THE VICINITY OF THE TARGET
- LINE IS VERY LONG IN TERMS OF TARGET SIZE, DISTANCE FROM LINE, AND WAVELENGTH
- LINE HAS A DISSIPATIVE LOSS $P_i \ell_t$ PER METER, OR D_T DECIBELS PER METER (Pi IS THE POWER LEVEL IN WATTS AT THE POINT IN THE LINE CONSIDERED)
- LINE RADIATES ENERGY OF $P_i \ell_r$ PER METER, OR D_R DECIBELS PER METER
- D_T AND D_R ARE SMALL ENOUGH THAT POWER GRADIENT ALONG THE LINE IS NOT VERY STEEP. THIS IMPLIES THAT THE RADIATION MAY BE CONSIDERED AS HAVING A CYLINDRICAL QUALITY

Figure 2 Conceptual Model of Bistatic Intrusion Radar

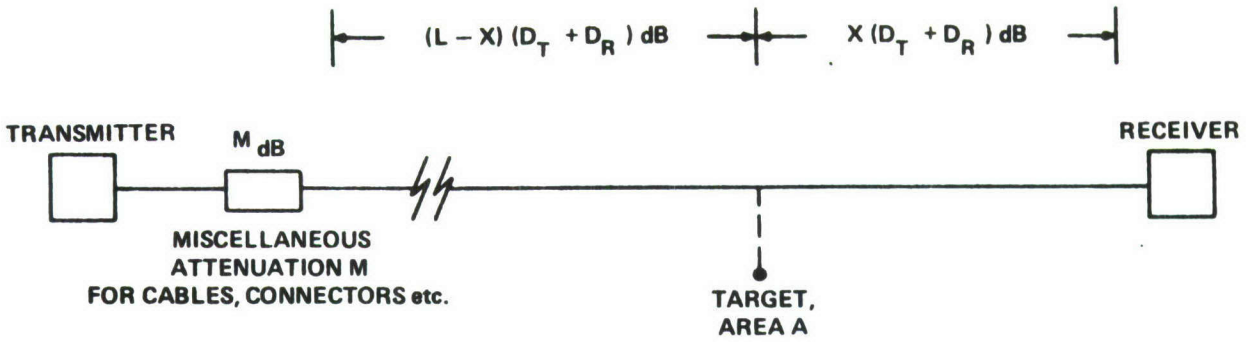

NOTE THAT $\left[(L - X)(D_T + D_R) + X(D_T + D_R) \right]$ dB = $\left[L(D_T + D_R) \right]$ dB AND THAT THE

TOTAL dB ATTENUATION ALONG THE LINE FROM THE TRANSMITTER TO THE RECEIVER IS:

$$\left[H + L(D_T + D_R) \right] \text{ DECIBELS}$$

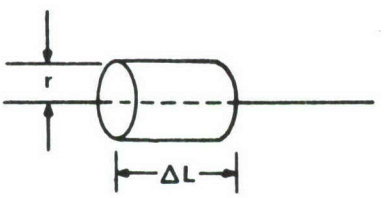

SURFACE AREA = $2\pi r\, \Delta L$

POWER RADIATED = $P_i \ell_r\, \Delta L$

ATTENUATION FROM LINE TO TARGET TO LINE IS FOUND TO BE $8.39 \dfrac{D_R^2 A}{r^2 F^2}$

D_R = dB/METER RADIANS

r = TARGET DETECTOR (METERS)

F = FREQUENCY IN MHz

WHEN THIS IS ALL ASSEMBLED IN DECIBEL FORM THE SIGNAL AT THE RECEIVER WHICH IS DUE TO THE TARGET IS S DECIBELS BELOW THE TRANSMITTER POWER WHERE S IS GIVEN BY:

$$S = \left[(-LD_R - LD_T - M + 9.2) + 10 \log \frac{A}{F^2} + 10 \log \frac{1}{r^2} + 20 \log D_R \right] \text{ DECIBELS}$$

Figure 3 An Overall Radar Equation for "Bistatic" Radar

TABLE 2

DETERMINATION OF OPTIMUM LINE RADIATION

- IN THE OVERALL EQUATION OF FIGURE 3 THE ONLY TERMS IN WHICH D_R APPEARS ARE $-LD_R$ AND $20 \log D_R$. THUS, INDEPENDENT OF ALL OTHER ELEMENTS, S WILL BE A MAXIMUM IF $S_{RF} = LD_R + 20 \log D_R$ IS A MAXIMUM

- S_{RF} WILL BE A MAXIMUM IF $\frac{dS_{RF}}{dD_R} = 0$, AND THIS IS FOUND TO OCCUR WHEN

$$D_R = \frac{20}{L \ln 10} = \frac{8.69}{L} \text{ DECIBELS}$$

$$\text{OR } D_R L = 8.69 \text{ dB}$$

- 8.69 dB FOR TOTAL LINE RADIATION GIVES THE OPTIMUM AVAILABLE SENSITIVITY FOR ANY CHOSEN LINE LENGTH REGARDLESS OF WHAT THAT LENGTH IS

NOTE: 8.69 dB CORRESPONDS TO A FACTOR OF 76% POWER

2. Goubau lines, with perturbations in the form of physical discontinuities introduced to increase its radiative qualities. Successful results obtained with Goubau lines are presented.

3. Twin Lead lines, with physical perturbations introduced to increase its radiative qualities. Successful results obtained with the twin lead lines are also presented.

In determining the radiative qualities of these perturbed lines the initial step was to measure the transmission characteristic of the line from end to end before the introduction of the physical perturbations. A second measurement was then made after the perturbations had been introduced into the line, and the additional end to end attenuation observed was attributed to radiation from the line. In every case, a coupling element and tunable matching unit was used at the input end of the line to deliver maximum power to the line from the transmitter employed. Only a coupling unit was used at the output end. While it might have been desirable to also provide matching at the output end in each case, it was not deemed essential. The approximations involved in the assumption that simple subtraction of the two attenuations observed gives the true radiative quality of the line probably introduces more inaccuraracies than the lack of matching at the output end. (The Aerospace Research Inc. radar transmitter discussed later in connection with Figure 8 (page 15) was used as a signal generator for these attenuation measurements.)

Perturbations to induce radiation in the Goubau line were provided by a slotted plastic plate through which the line could be looped, and a plastic grooved cylinder to maintain the dimensions of the loop. In the case of the twin lead line perturbations were introduced by plastic spacing rods longer than the normal line spacers which were inserted periodically

to increase the spacing of the conductors at regular intervals. The plastic pieces used to introduce the physical discontinuities in the line were not believed to introduce significant additional dissipative loss.

Figure 4 is a photograph of two Goubau line sections showing two different sizes of perturbing elements inserted. Figure 5 is a photograph of the twin lead line with and without the perturbing elements. In each photograph a one dollar coin is shown for size reference.

4. TEST ARRANGEMENT

Tests of the line in conjunction with a radar type detector were made by use of an Aerospace Research Incorporated radar unit furnished by the government. The performance of the ground clutter balancing mechanism of this radar was not sufficiently effective against the clutter appearing in these line tests to permit using the overall radar directly in the sensitivity measurements. Therefore, the signal processing portion of the radar was by-passed and measurements were made directly from the coherent detection system through the band pass amplifier portion of the radar unit.

A sufficiently large target was used to permit direct signal observation in the presence of the clutter. The test target was provided with an oscillating mechanism whose stroke was adjusted so that the movement of the target over an oscillation cycle was slightly over 1/2 wavelength at the 915 MHz frequency, corresponding to a range change with respect to the line of slightly over one wavelength. Thus, all possible phase positions for the coherent detector output were covered by the movement of the target, thereby assuring that the peak to peak oscilloscope deflection observed

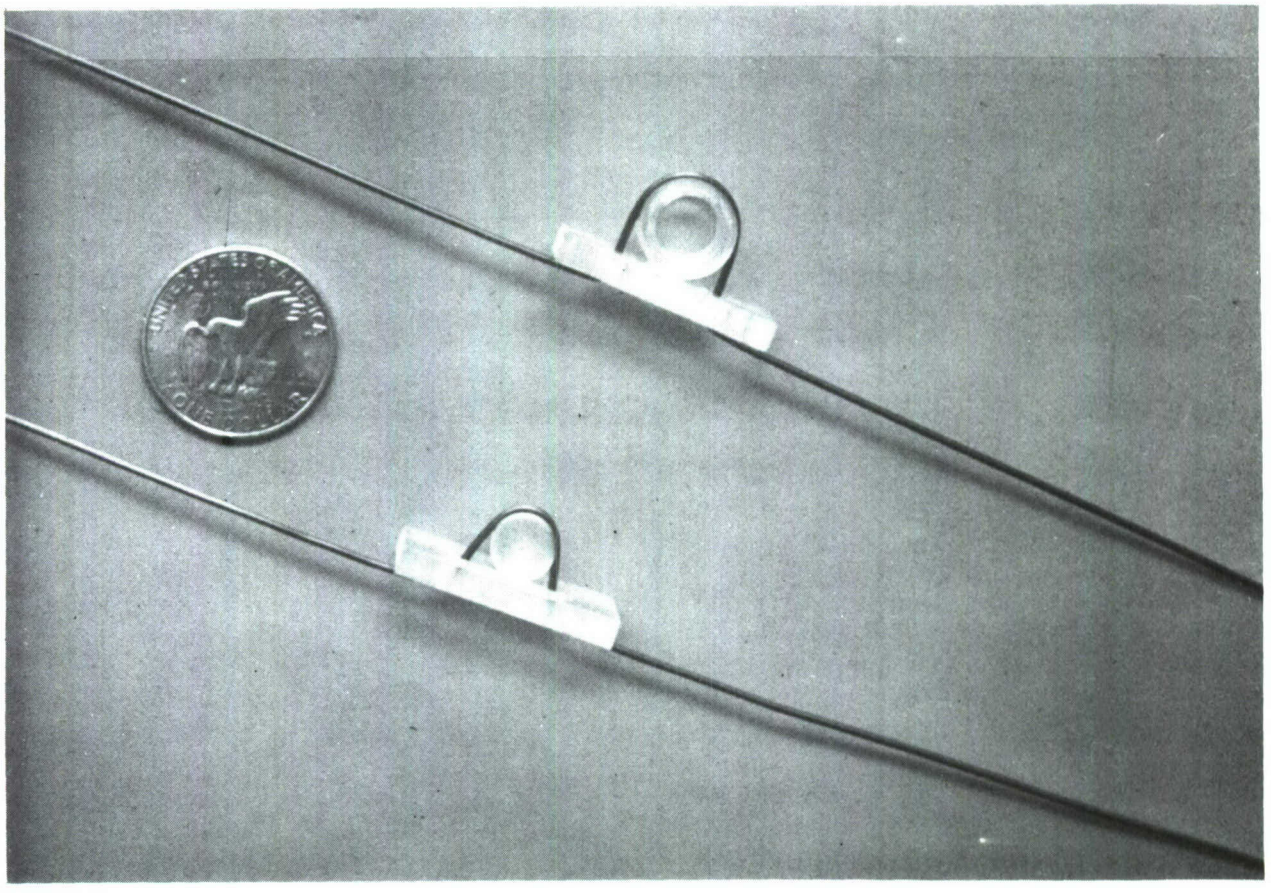

Figure 4 Discontinuities Introduced in Goubau Line to Increase Radiation

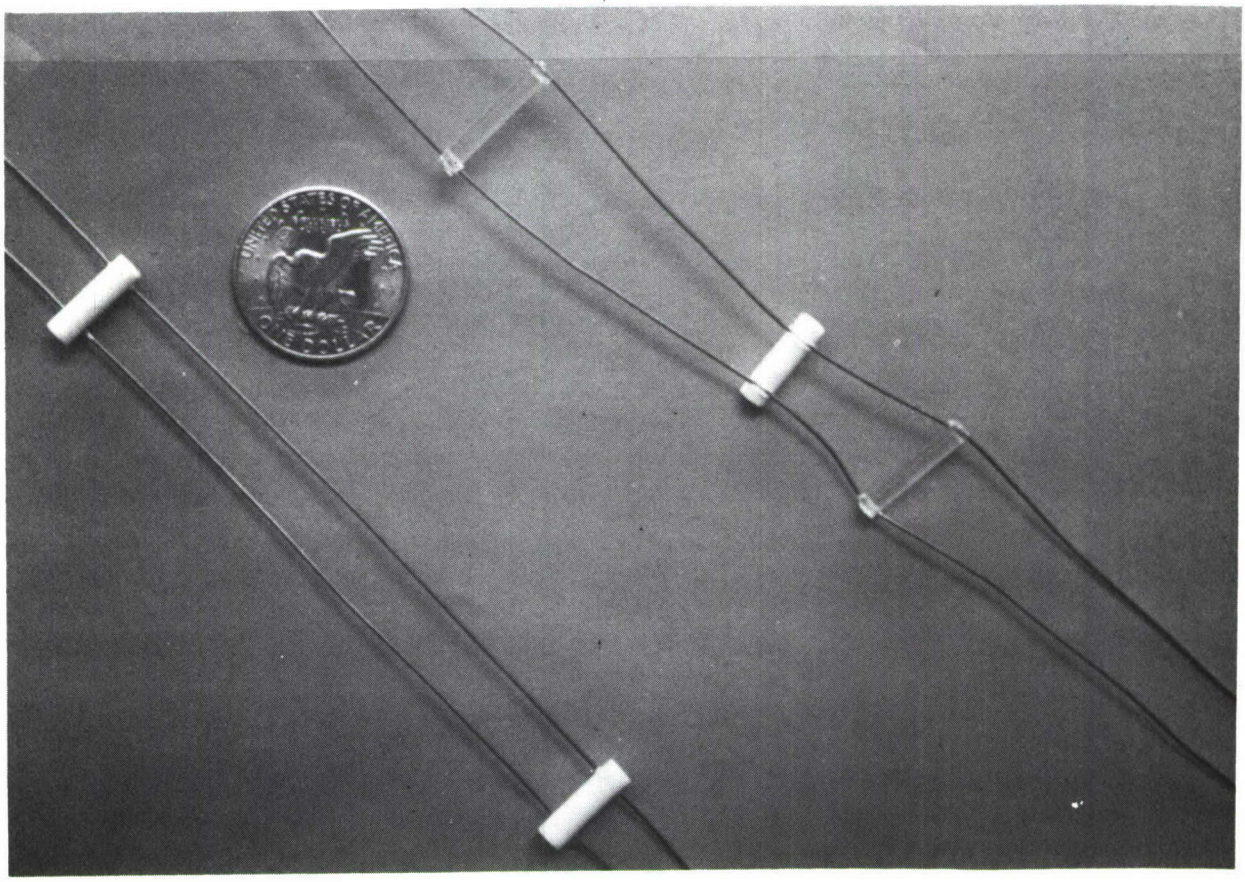

Figure 5 Unmodified Twin Lead and Discontinuities Added to Increase Radiation

represented the full value of the signal reflected from the moving test target. The stroke was kept relatively small (±3") compared to the range of measurement so that a single average range could be applied to the oscillating target with insignificant error. This device is illustrated in Figure 6.

In making the measurements with the radar unit and a relatively short length of test line it was possible to simulate the full length of a desired line by adding to the receiver input circuit an attenuation which would correspond to the additional loss (including radiation) which would occur in such a full line length. This simulation of full length line is satisfactory with respect to measurement of radar sensitivity but it is not simulative of the full clutter input to the radar since the attenuation representing additional line does not include the clutter which would exist with a real full length line. This situation and examples of its magnitude are illustrated in Figure 7.

A detailed block diagram of the radar sensitivity measurements system is shown in Figure 8. The receiver sensitivity was calibrated by connecting the high gain DC coupled oscilloscope directly to the output of the double balanced modulator and observing the deflection level change caused by introducing calibrated attenuation into the input signal. The sensitivity measurements were then made through the band-pass amplifier which had been separately calibrated. The target oscillation rate was set to correspond to a frequency of approximately 1/3 Hz which is well within the pass-band of the amplifier.

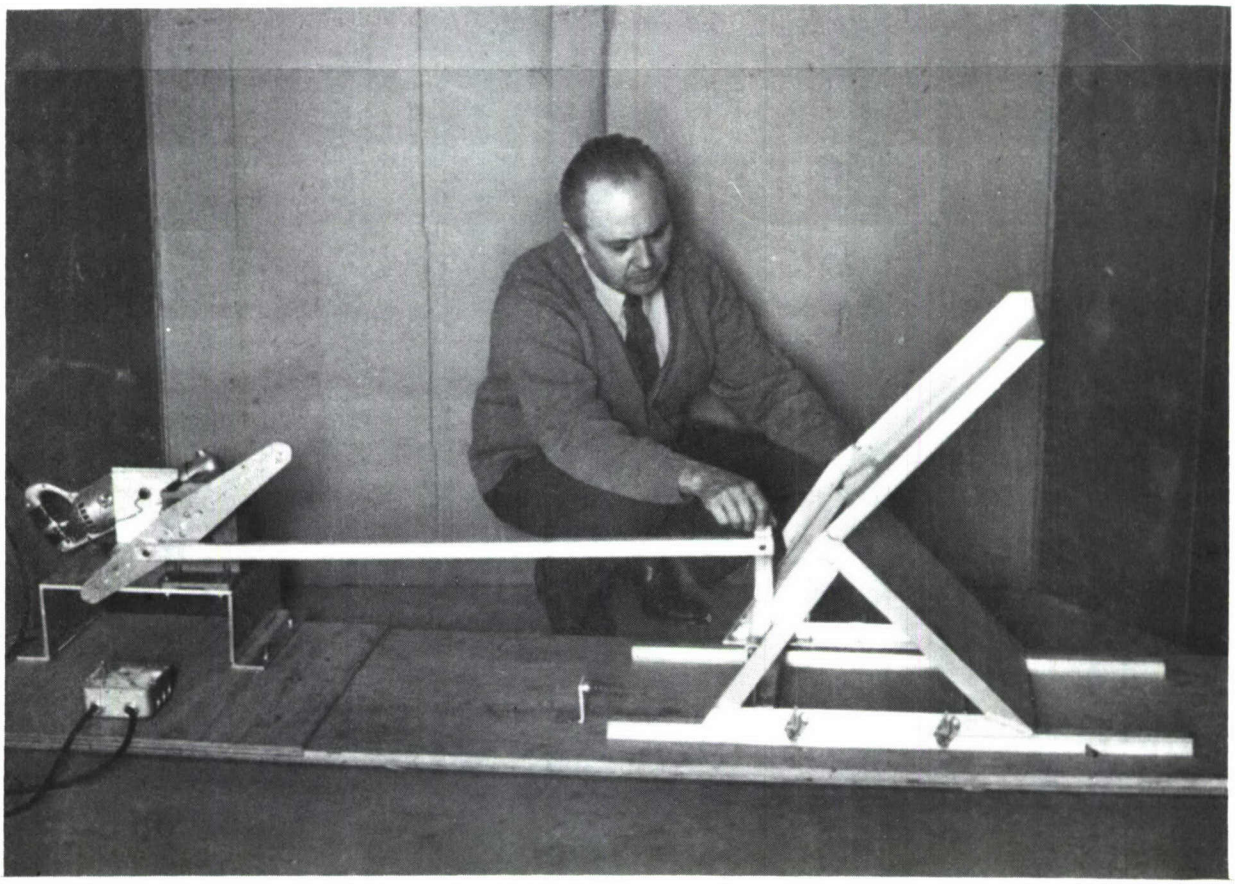

Figure 6 Moving Target Simulator for Test of Intrusion Line Radar

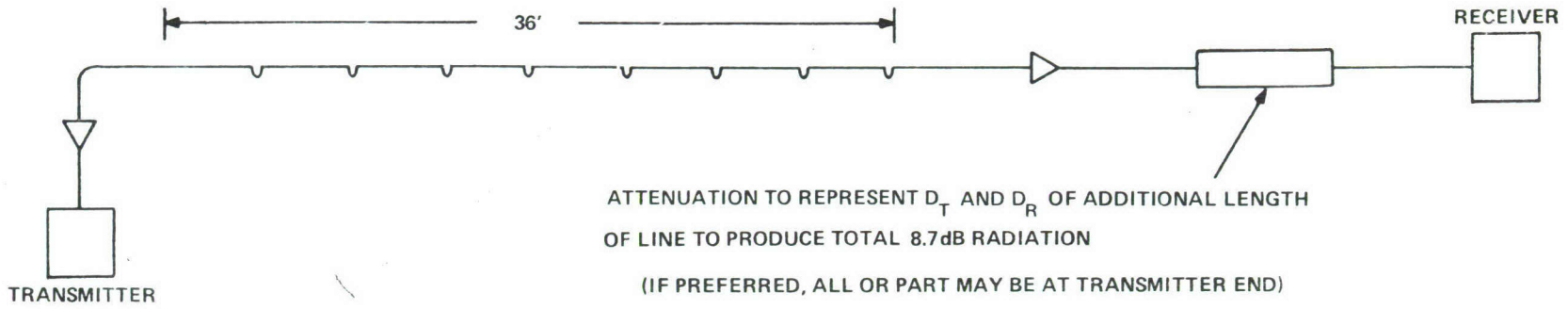

- FOR FIRST GOUBAU LINE RADIATION IS 1.2 dB FOR 36 ft, OR 0.11 dB/m
- LENGTH OF LINE FOR FULL 8.7 dB RADIATION IS 261 ft, OR 225 ft (68.8 m) IN ADDITION TO THE 36 ft SHORT LENGTH
- FROM FIGURE 9, $D_T = 0.036$, $D_R = 0.11$ dB/m. ADDITIONAL ATTENUATION TO SIMULATE 68.8 ADDITIONAL METERS LENGTH IS 68.8 (0.11 + 0.036) = 10.0 dB
- NOTE THAT SIMULATED LINE DOES NOT SIMULATE FULL CLUTTER VALUE. IN THIS CASE 36 ft LENGTH HAS ONLY $\frac{36}{261} = 0.138$ THE CLUTTER POWER LEVEL OF THE FULL LENGTH LINE. FULL LENGTH LINE CLUTTER WILL BE $\frac{261}{36} = 7.25$ TIMES AS GREAT, OR 8.6 dB GREATER

Figure 7 Simulation of a Long Line by Use of a Short Section and Auxiliary Antenna

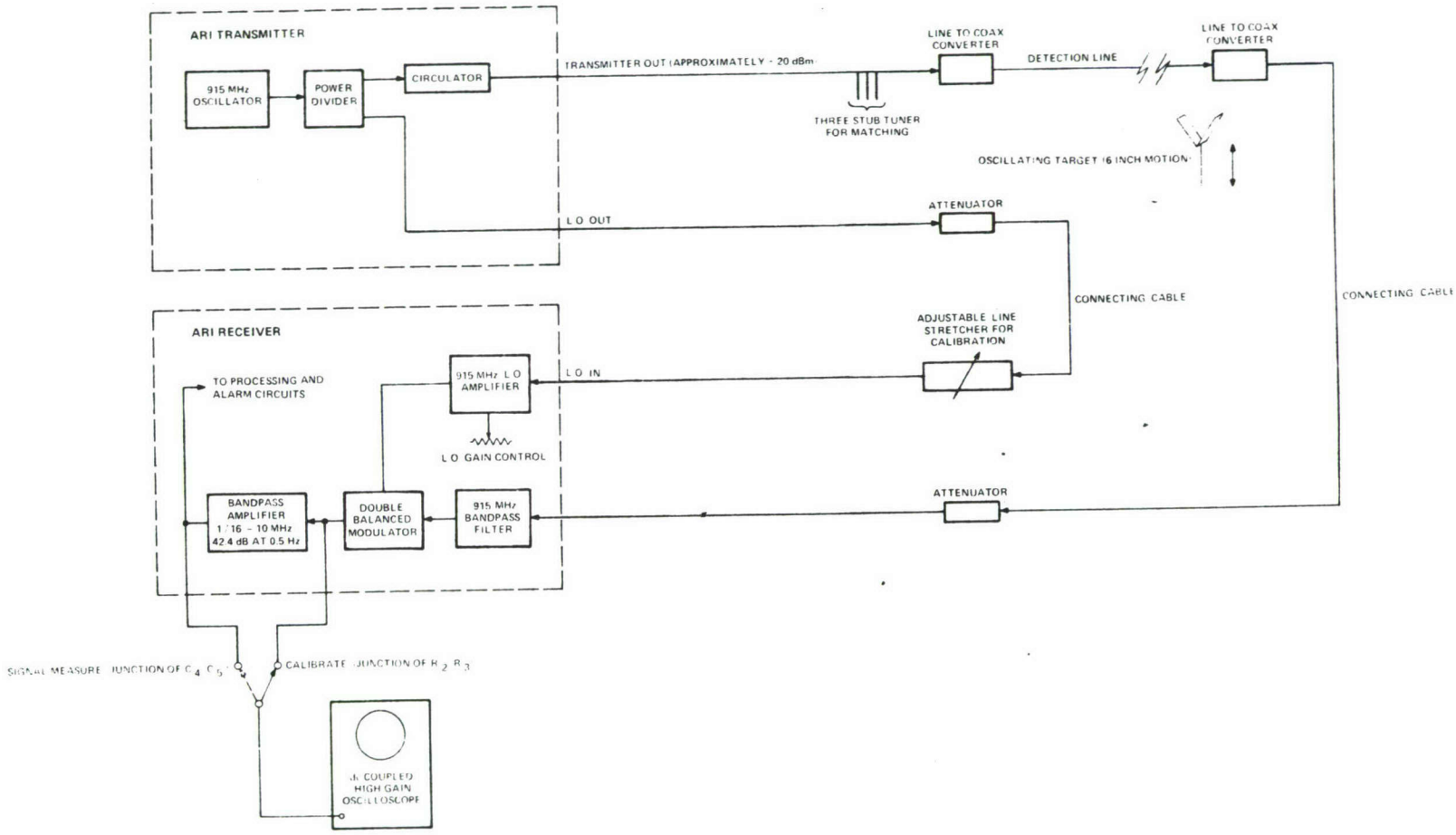

Figure 8 Block Diagram of Signal Measurement System Using ARI Radar Transmitter and Receiver (Processing and Alarm Elements Not Used)

5. TEST RESULTS

The results obtained in tests of these lines with several dimensions of the perturbing elements are shown in Figure 9, along with the general test arrangement. In each case the length of line which will give 8.69 dB overall radiated loss is shown. The data for Figure 9 have been compiled in tabular form in Table 3. It should be realized that these line lengths calculated are those for which the radiation factor is most suitable. This optimization is not very critical however, and rather large deviations may be made from the optimum radiation factor without materially reducing the radar sensitivity. This is illustrated in Figure 10 which shows the sensitivity measure of the radar as a function of the radiation factor for those typical line lengths. Referring to Figure 10 and the curve shown for 50 meters line length, it will be seen that the radar sensitivity measure is only about 1 dB below optimum over the entire range of radiative factors from 0.1 dB per meter to 0.3 dB per meter where the specific optimum value for radiation is 0.174 dB per meter. (Appendix A, gives further discussion of this matter in connection with Figure 7 of the appendix which is the same as Figure 10 in the letter report proper.)

In order to present the results obtained in relation to the analytic model used, the results predicted were calculated and plotted in graphical form. The results actually measured were then plotted in the graphical presentation so that their relationship to the predicted results may be seen. Examples of the calculation of expected results are shown in Table 4.

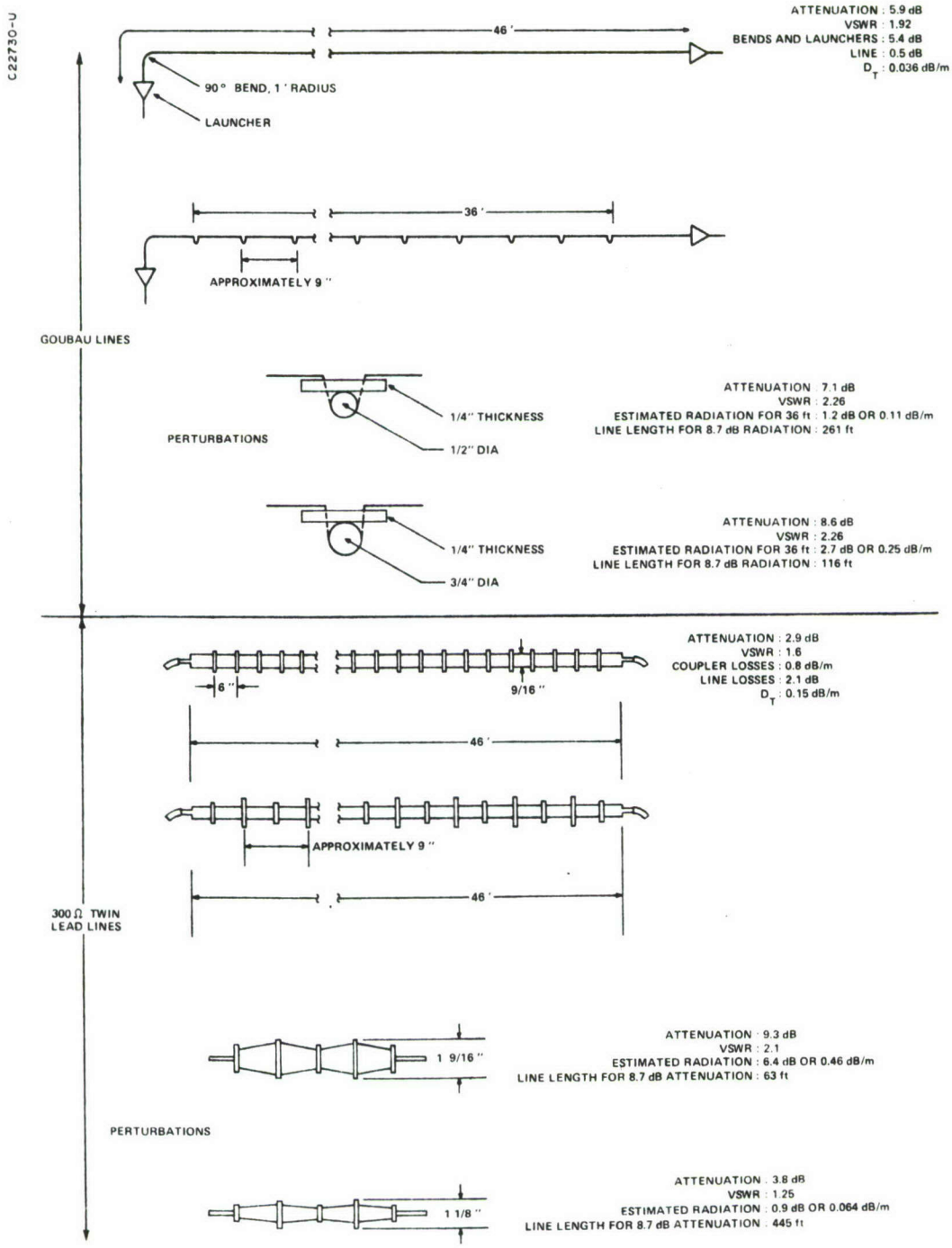

Figure 9 Lines and Line Perturbation Methods

TABLE 3

SUMMARY OF DISSIPATIVE AND RADIATION LOSSES OF LINES

B22736-U

LINE DESCRIPTION	COXIAL LINE TO OPEN – LINE LOSS – TOTAL FOR TWO COUPLERS (dB)	90° BEND LOSS (dB)	LINE DISSIPATIVE LOSS FOR 46 ft (dB)	EXCESS RADIATION LOSS FOR PERTURBED LENGTH (dB)	INPUT VSWR	D_T DECIBEL/METER (dB/m)	EXCESS D_R DECIBELS/METER (dB/m)	LINE LENGTH FOR 8.7 dB RADIATION (ft)
GOUBAU LINE 46' UNPERTURBED	3.0	2.4	0.5	——	1.9	0.036	——	——
GOUBAU LINE 46' WITH 36' PERTURBED $\frac{1}{2}$"	3.0	2.4	0.5	1.2	2.3	0.036	0.11	261
GOUBAU LINE 46' WITH 36' PERTURBED $\frac{3}{4}$"	3.0	2.4	0.5	2.7	2.0	0.036	0.25	116
300Ω TWIN LEAD LINE WITH 46' UNPERTURBED	0.8	——	2.1	——	1.6	0.15	——	——
340Ω TWIN LEAD LINE WITH 46' PERTURBED	0.8	——	2.1	6.4	2.1	0.15	0.46	63
300Ω TWIN LEAD LINE WITH 46' PERTURBED FULL LENGTH 1 $\frac{1}{8}$"	0.8	——	2.1	0.9	1.25	0.15	0.064	445

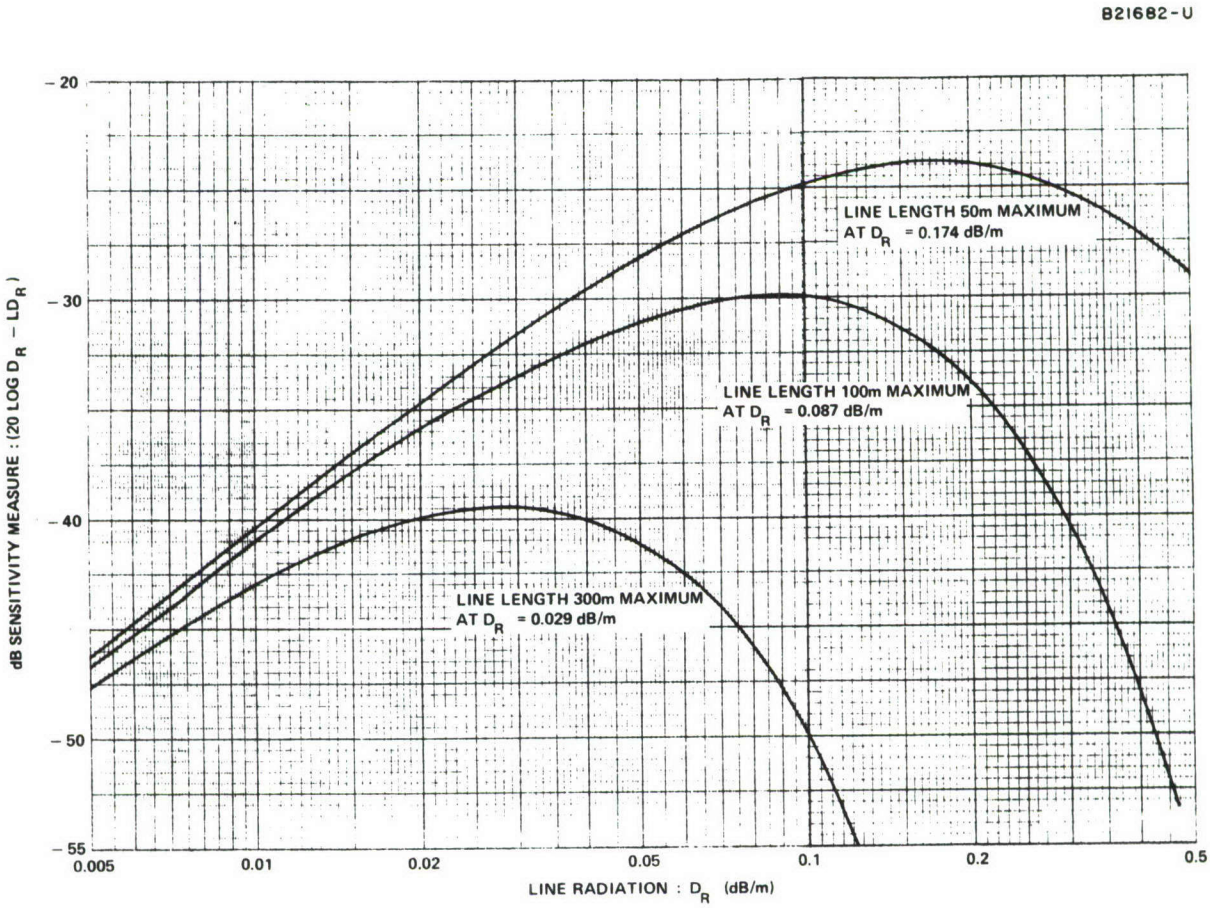

Figure 10 Sensitivity Measure as a Function of Line Radiation in a Bistatic Line Intrusion Detector

TABLE 4

PREDICTED TEST RESULTS WITH OSCILLATING TARGET

C22738-U

$$S = 10 \log \frac{A}{F^2} + 20 \log D_R + \overbrace{(-LD_R - LD_T - M + 9.2)}^{B} + 10 \log \frac{1}{r^2}$$

FOR PERTURBED GOUBAU LINE ($\frac{1}{2}$" DIA PERTURBERS)

$10 \log \frac{A}{F^2} = -49.2$ dB — $A = 10\ m^2$; $F = 915$ MHz

$20 \log D_R = -19.2$ dB — $D_R = 0.11$ dB/m

$B + 9.2 = -12.0$ dB — $B = 21.2$ dB (MEASURED)

$S = 10 \log \frac{1}{r^2} - 80.4$ dB

$P_R = \left[10 \log \frac{1}{r^2} - 60.2\right]$ dBm — $P_R = P_T + S$; $P_T = 20.2$ dBm (MEASURED)

FOR PERTURBED TWIN LEAD LINE ($1\frac{9}{16}$" PERTURBERS)

$10 \log \frac{A}{F^2} = -49.2$ dB — $A = 10\ m^2$; $F = 915$ MHz

$20 \log D_R = -6.7$ dB — $D_R = 0.46$ dB/m

$B + 9.2 = -14.4$ dB — $B = 23.6$ dB (MEASURED)

$S = 10 \log \frac{1}{r^2} - 70.3$ dB

$P_R = \left[10 \log \frac{1}{r^2} - 50.1\right]$ dBm — $P_R = P_T + S$; $P_T = 20.2$ dBm (MEASURED)

FOR PERTURBED TWIN LEAD LINE ($1\frac{1}{8}$" PERTURBERS)

$10 \log \frac{A}{r^2} - 49.2$ dB — $A = 10\ m^2$; $F = 915$ MHz

$20 \log D_R = -23.9$ dB — $D_R = 0.064$ dB/m

$B + 9.2 = 8.7$ dB — $B = 17.9$ dB (MEASURED)

$S = 10 \log \frac{1}{r^2} - 81.8$ dB

$P_R = \left[10 \log \frac{1}{r^2} - 50.1\right]$ dBm — $P_R = P_T + S$; $P_T = 20.2$ dBm (MEASURED)

TABLE OF PREDICTED TEST RESULTS

r RANGE (m)	$10 \log \frac{1}{r^2}$ (dB)	RECEIVED LEVEL (dBm)	
		PERTURBED GAUBAU LINE $D_R = 0.11$ dB/m	PERTURBED TWIN LEAD LINE $D_R = 0.46$ dB/m
1.0	0	– 60.2	– 50.1
1.5	– 3.5	– 63.7	– 53.6
2.0	– 6.0	– 66.2	– 56.1
2.5	– 8.0	– 68.2	– 58.1
3.0	9.5	– 69.7	– 59.6
4.0	12.0	– 72.2	– 62.1
5.0	13.9	– 74.1	– 64.0

The data of Table 4 have been expanded and plotted smoothly in Figure 11, along with the results actually obtained with the test arrangement of Figure 8. These actual results have been connected by point to point line plots. It will be seen that none of the actual measurements closely follow the predicted results, but, on the other hand, they do fall in the same general range; it is believed that these results constitute reasonable validation of the model.

The model conceives of a situation in free space with no significant reflections. On the other hand, the measurements were made with both ground and walls relatively close to the line antenna with large reflections probable from these adjacent flat surfaces. The tests were performed in a garage-like area with the floor ranging from 3 to 8 feet from the line and with the walls about 12 feet from the line.

It will be noted by an examination of Figure 11 that there is a marked similarity in the general plots of the actual returns obtained from three of the lines, namely; the unperturbed twin lead line, the 0.064 dB per meter perturbed twin lead line, and the 0.11 dB per meter Goubau line. This may well be due to reflective factors which similarly affect all of the lines with relatively low radiation factors. (The "non-perturbed" twin line has some noticeable but unevaluated low radiation factor due in part to the discontinuities introduced by the line spacers). The lines which have the large radiation factors may be so drastically perturbed as to have irregularities of their own which mask the basic sensitivity pattern exhibited by the lines having lower radiative values.

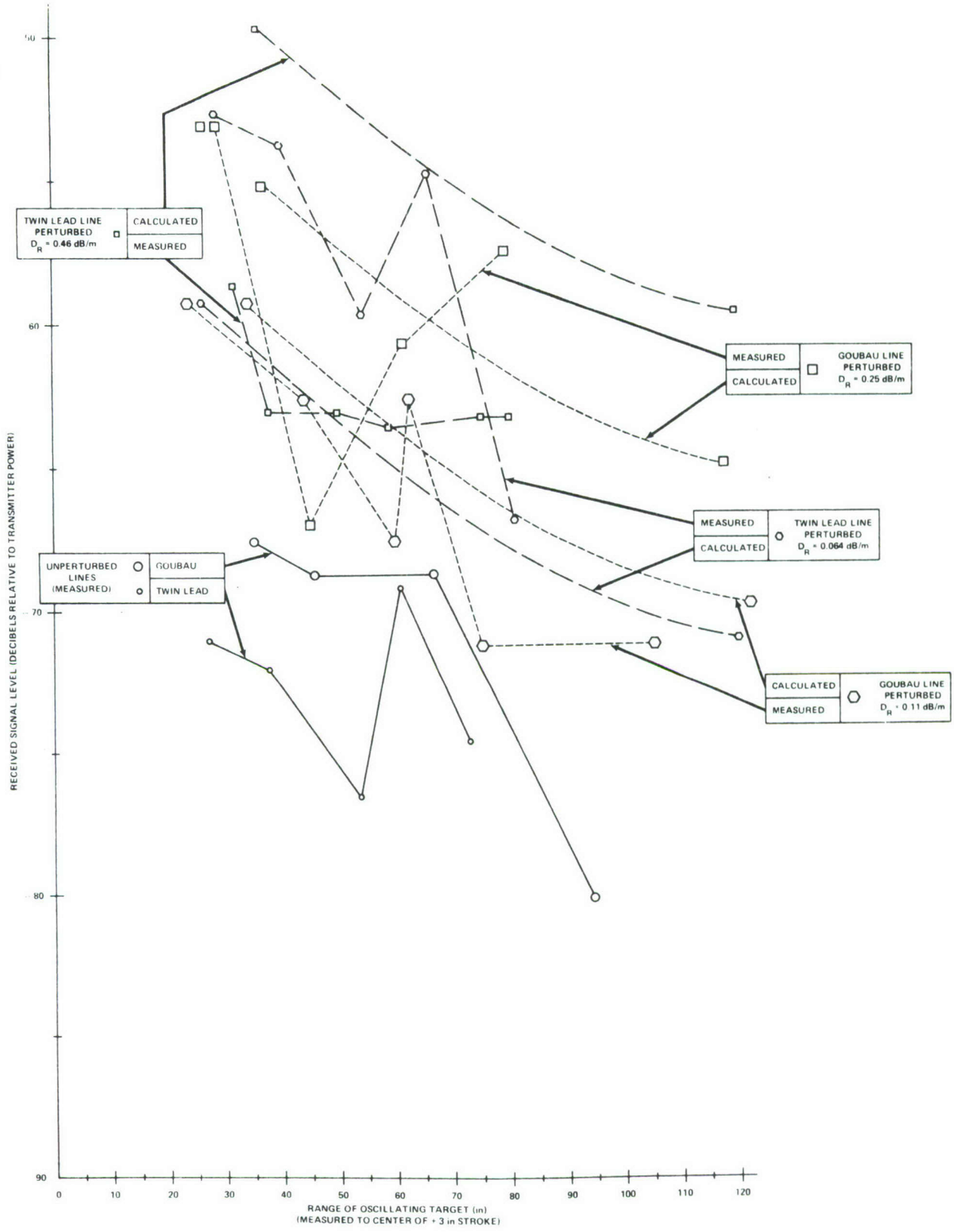

Figure 11 Plot of Actual and Predicted Results

This matter has not been examined in analytic depth, but it is considered that the similarity of the shape of the lower radiation factor lines is so striking as to be particularly noted.

It is beyond the scope of this investigation to evaluate the performance of the ARI radar unit which was used in conjunction with the line. The ARI unit was designated by the manufacturer as "ADVISOR X" but it differed from the company's standard units of this type in having a separate receiver enclosure to allow placement of the receiver at the end of the line antenna opposite from the transmitter end. Some casual experiments were performed as to the radar unit's performance, and the observations will be reviewed here. It was noted that, if the line remained very stationary, and, with critical adjustment of the balancing system, quite consistent detections could be obtained of a man walking under the line which was located 8 to 10 feet above the floor at the point of test. This was true even for a crawling person moving relatively slowly, although on some occassions detection of this type motion was missed. However, even extremely small motions of the line antenna produced large spurious outputs in the system, resulting in false intrusion alarms. Under this condition it was necessary to set the threshold adjustment below levels at which satisfactory detection was obtainable.

Development of a clutter model and clutter measurements were not within the scope of the contract, but it appears that clutter reflections set a very serious restriction on the use of this instrument, and that some type of embedding or very rigid restraint of the line would be required for its use without a substantial improvement in radar clutter rejection.

6. CONCLUSIONS

It appears that the sensitivity model developed for the performance of a line radar as illustrated in Figure 1 is suitable for determination of the general magnitude of target echoes to be expected.

It is also concluded that perturbations of various kinds applied to basically uniform transmission lines can produce a radiative quality of the general type required for a radar of this kind.

A further conclusion is that the clutter in such a system as this represents a very major input to the detecting system, since movement of the line causes movement of the entire clutter pattern. This situation presents a discrimination requirement which is much more severe than that which is encountered in systems in which the transmit and receive antennas remain truly stationary and where the relative clutter motion involves only the movement of the clutter sources.

7. RECOMMENDATIONS

A considerable amount of additional work is recommended directed to determination of the optimum methods to be used for perturbing uniform lines of the types tested here. Since the best overall performance appeared to be available from the line showing the smallest standing wave ratio and the smallest explicit radiation in dB per meter it seems evident that a more exhaustive investigation should be undertaken to determine the best possible configuration with respect to these factors. (The 0.064 dB/meter radiation twin line appears to be the most satisfactory of those represented in Figure 11.)

A second recommendation is that the matter of clutter returns produced in such a system be examined in greater depth and that a more accurate model be created and verified by controlled experiments.

A third recommendation is that further examination be made of the qualities of the balanced processing circuits to be used for radars of this type.

8. DELIVERED ITEMS

The delivered items required have been furnished as follows:

Goubau Line

2 Coupling Horns

1 Roll # 14 wire, approximately 1200'

100 perturbing elements (3/4" cylinders and matching plates - See Figure 4)

100 perturbing elements (1/2" cylinders and matching plates - See Figure 4)

Twin Lead Line

1 Roll standard 300 ohm twin lead line, length approximately 500'

200 Perturbing rods - 1 1/8" length (See Figure 5)

200 Perturbing rods - 1 1/2" length (See Figure 5)

The perturbing elements may be assembled as shown in Figures 4 and 5. It is expected that a small amount of plastic cement may be applied to each spacer end to secure the twin-lead spacers if necessary. Dimensions are not critical, and additional pieces may be made if desired, using as samples the pieces provided.

APPENDIX A

DERIVATION OF RANGE EQUATIONS FOR LINE INTRUSION DETECTOR AND LINE DESIGN OPTIMIZATION

SURC TN-73-373

E.K. Stodola

28 November 1973

DERIVATION OF RANGE EQUATIONS FOR LINE INTRUSION DETECTOR AND LINE DESIGN OPTIMIZATION

E. K. Stodola

SYRACUSE UNIVERSITY RESEARCH CORPORATION

GENERAL

These equations are derived using the same general approach used for the derivation of conventional radar equations.*

The intrusion detector consists of a transmission line which, in addition to its normal dissipative loss also radiates a significant fraction of the power applied to it , along with a transmitter, receiver, and indicators.

BISTATIC INTRUSION DETECTION RADAR

In one configuration the transmitter is located at one end of the line and the receiver at the other, as illustrated in Figure 1.

Figure 1

The line loses ℓ_t per meter of line length of the applied power at any point, and radiates ℓ_r per meter of line length of the applied power. The radiation from the line is small enough so that the radiated field can be considered as cylindrical with a slowly tapering power level from the transmitter to the receiver.

If a target is moved radially in the field the Doppler effect creates a signal at a shifted frequency which is induced in the line and proceeds from the induction point to the receiver (with an equal portion going toward the transmitter which is ignored for the moment).

*Such a derivation is given in an earlier paper "Detection of Radio Signals Reflected from the Moon", J.H. DeWitt, Jr. and E. K. Stodola, Proc. of the IRE p 229, March 1949. Appendix I includes the relevant section of this paper and a brief discussion of a minor difference in the derivation used here.

Assuming the process to be linear, the ratio of the target signal to the transmitted level in the line at the point adjacent to the target is a fixed ratio dependent upon the target size, reflectance, and distance r from the line.

Since the total attenuation (due to both dissipation and radiation) along the line is fixed, and the attenuation from the line to the target and back is also fixed and additive to this, the sensitivity of the system is independent of where <u>along</u> the line the target is introduced.* Other arrangements are possible and their performance can be determined as long as the ratio of the signal induced in the line to the power level in the line is known.

This ratio will now be determined. Consider a line as in Figure 2 with a cylindrical field and with an isotropic receiving antenna at a distance r from the line, and with a power level of p_i flowing along the line at the point being considered.

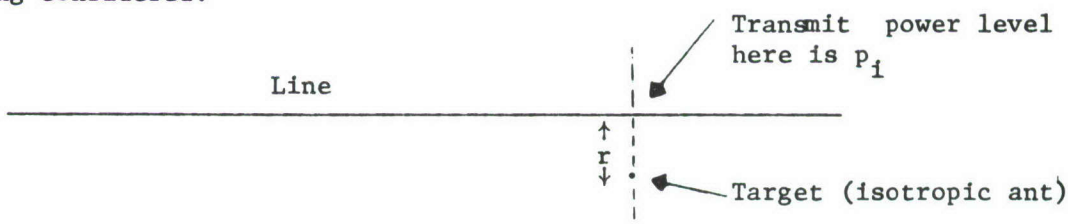

Figure 2

Assume an elementary line segment of length ΔL (Figure 3).

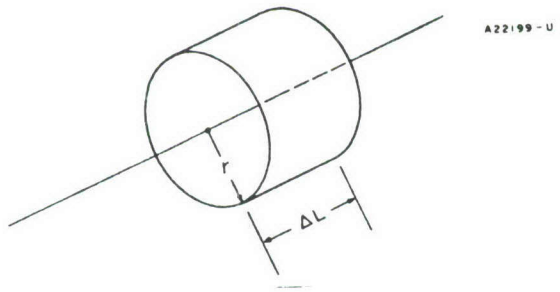

Figure 3

*The constant sensitivity quality of this radar configuration was shown in a different type analysis by Dr. Theodor Tamir as a consultant to SURC.

The power radiated is $p_i \ell_r \Delta L$, and the area through which this is radiated is $2\pi r \Delta L$, giving a power density at the radius r of

$$\frac{p_i \ell_r \Delta L}{2\pi r \Delta L} = p_i \frac{\ell_r}{2\pi r} \text{ watts/square meter} \quad (1)$$

Consider that the target is an isotropic antenna which will absorb power from the line and then reradiate in all directions. This is a characteristic of a typical scatterer, but considering it as an antenna facilitates the reasoning.

The effective area of a receiving antenna is

$$A_r = \frac{G_r \lambda^2}{4\pi} \text{ square meters} \quad (2)$$

where G_r is the gain with respect to an isotropic antenna and λ is the wavelength in meters

If F is the operating frequency in megahertz,

$$\lambda = \frac{300}{F} \text{ meters,}$$

combining these gives

$$A_r = 7160 \frac{G_r}{F^2} \text{ square meters} \quad (3)$$

For this case of the isotropic antenna, $G_r = 1$, and

$$A_r = \frac{7160}{F^2} \text{ square meters} \quad . \quad (3a)$$

If the power density at radius r (Eq. 1) is applied to this area the received power at the target, p_t is

$$P_t = p_i \frac{\ell_r}{2\pi r} \times \frac{7160}{F^2} = \frac{1141\ \ell_r}{r\ F^2} \qquad (4)$$

If this power is frequency shifted and transmitted back toward the line from the isotropic antenna, it will undergo the same attenuation, since the network is bilateral.* This will make the signal p_r returning toward the transmitter end of the line, (and by symmetry, toward the receiver end of the line)

$$p_r = p_i \left(\frac{1141\ \ell_r}{r\ F^2}\right)^2 = 1.303 \times 10^6\ \frac{\ell_r^2}{r^2\ F^4} \qquad (5)$$

The above calculation is an exact analogue for the situation of a lossless target of the scattering area of an isotropic antenna. For the actual effective echoing area A involved, the power of (5) must be multiplied by the ratio of the actual echoing area to the effective area of an isotropic antenna (Equation 3a).

$$\frac{A}{A_r} = \frac{A\ F^2}{7160} \qquad (6)$$

and, multiplying (5) by this factor gives

$$p_r = p_i\ 1.303 \times 10^6\ \frac{\ell_r^2}{r^2 F^4} \cdot \frac{A\ F^2}{7160}$$

$$= p_i\ 1.585 \times 10^2\ \frac{\ell_r^2\ A}{r^2\ F^2} \qquad (7)$$

It will be noted that the factor ℓ_t, the line transmission loss does not

*Appendix 2 shows the application of this principle to a simple resistive network to illustrate the concept involved.

appear in this equation. However, it does enter the system performance equations since it will attenuate the transmission from the transmitter to the point on the line nearest to the target, and from this same point on the line to the receiver.

Referring to (7), the "gain" K from line transmit, to target, to line receive, can be written as

$$K = \frac{P_r}{P_i} = 1.585 \times 10^2 \frac{\ell_r^2 A}{r^2 F^2} \tag{8}$$

To indicate the magnitudes involved, assume

Target Area A = 1 square meter

Frequency F = 915 MHz

Line radiation of 10 dB/100 meters, .1 dB/meter, which corresponds approximately to $\ell_r = 0.023$.

Distance of target from line,

$r = 3$ meters .

$$K = 1.585 \times 10^2 \frac{(.023)^2 \times 1}{3^2 \times 915^2} = 1.12 \times 10^{-8} , \tag{9a}$$

which corresponds to

$$-79.5 \text{ dB} . \tag{9b}$$

If it be assumed that the line has a dissipative loss of 6 dB/100 meters and a line length of 300 meters is desired, the total attenuation from transmitter to receiver is

$$\frac{300}{100} (10 + 6) + 79.5, \text{ or } 127.5 \text{ dB} \tag{9c}$$

Thus, a radar unit is required which is capable of detection 127.5 dB below its transmitter level. This requirement is reduced by 16 dB for each 100 meters reduction in line length.

OPTIMIZATION OF LINE CHARACTERISTICS FOR BISTATIC CASE

The matter of setting an optimum value for ℓ_r will now be considered. Consider Figure 4 in which the line between the transmitter and receiver is shown.

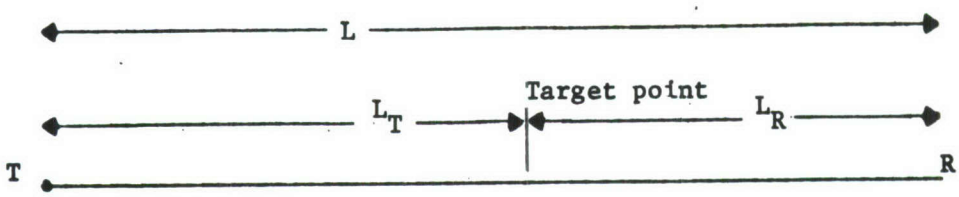

Figure 4

D_T = line attenuation in dB/meter for dissipative (transmission) loss

D_R = line radiation "loss" in dB/meter

D_c = Total attenuation for signals passing along the line $D_T + D_R$ in dB/meter

The relation of loss factor ℓ per unit length to dB attenuation per unit length is as follows:

$$10^{\frac{-D}{10}} = 1 - \ell, \quad \ell = 1 - 10^{\frac{-D}{10}} \tag{10}$$

This relation has been plotted in Figure 5, it will be seen that for the range of values considered of interest in this analysis the relation of A to ℓ is very nearly linear, and, by scaling is found to be

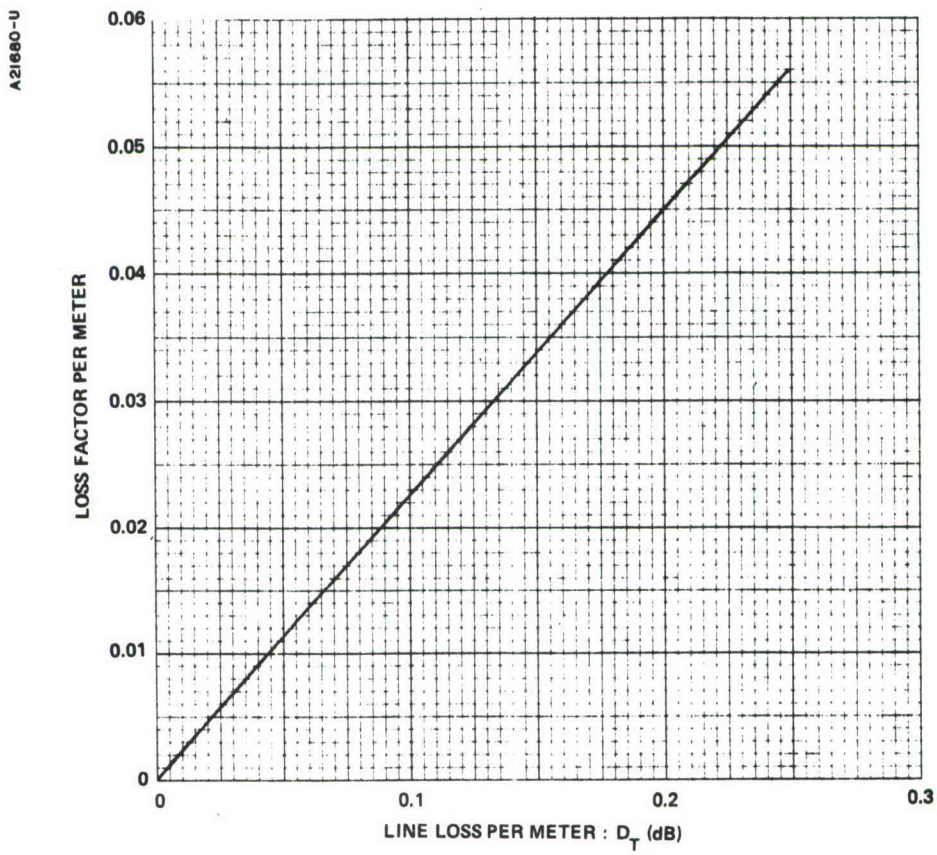

Figure 5 Relation of Loss Factor ℓ to Loss in dB/Meter

$$\ell = .23\ D \tag{11}$$

It can be shown analytically that, for small values of ℓ, Equation (10) can be written as

$$\ell = \frac{\ln 10}{10}\ D$$

which is numerically equivalent to (11)

Referring to Figure 4, it will be seen that the attenuation from the transmitter to the target point (region) on the line is

$$L_T\ (D_T + D_R),$$

and the attenuation from the target point to the receiver is

$$L_R\ (D_T + D_R).$$

Since $L_T + L_R = L$, the total line length, the total attenuation from transmitter to receiver along the line is

$$L(D_T + D_R) \tag{12}$$

The additional attenuation in getting from the line to the target object and back is given by (8). This may be written in decibel form as

$$10 \log \frac{P_r}{P_i} = 10 \log 1.585 \times 10^2 + 10 \log \frac{A}{r^2 F^2} + 10 \log \ell^2$$

$$= 22.0 + 10 \log \frac{A}{r^2 F^2} + 10 \log \ell_r^{\,2} \tag{13}$$

It was noted in (11) that $\ell = .23\ D$, so applying $\ell_r = .23\ D_R$ to (13),

$$10 \log \frac{P_r}{P_i} = 22 + 10 \log \frac{A}{r^2 F^2} + 10 \log (.23 D_R)^2$$

$$= 9.2 + 10 \log \frac{A}{r^2 F^2} + 20 \log D_R \qquad (14)$$

Combining (12) and (14) with the proper signs gives the overall "gain", S from transmitter to receiver via the target as

$$S = - L D_R - L D_T - M^* + 9.2 + 10 \log \frac{A}{r^2 F^2} + 20 \log D_R \qquad (15)$$

In Equation (15) it will be noted that in the expression for "gain", S, from transmitter to target to receiver, only the first and last terms depend upon the line radiation per meter, D_R. The first of these terms decreases the gain as D_R increases while the other increases the gain as D_R increases. These two terms may be called the radiation factor S_R, and the other the target coupling factor, C_T, and,

$$S_R = - L D_R \text{ Decibels} \qquad (16)$$

$$C_T = 20 \log D_R \text{ Decibels} \qquad (17)$$

S_R becomes an intolerably large negative number if D_R is too large, and C_T becomes an intolerably large negative number if D_R is too small. In Figure 6

---

*Any negative gain (loss) inconnections and line couplers from transmitter and receiver to the line ends must be included in the total value of S. This loss is designated by M in Equation (15).

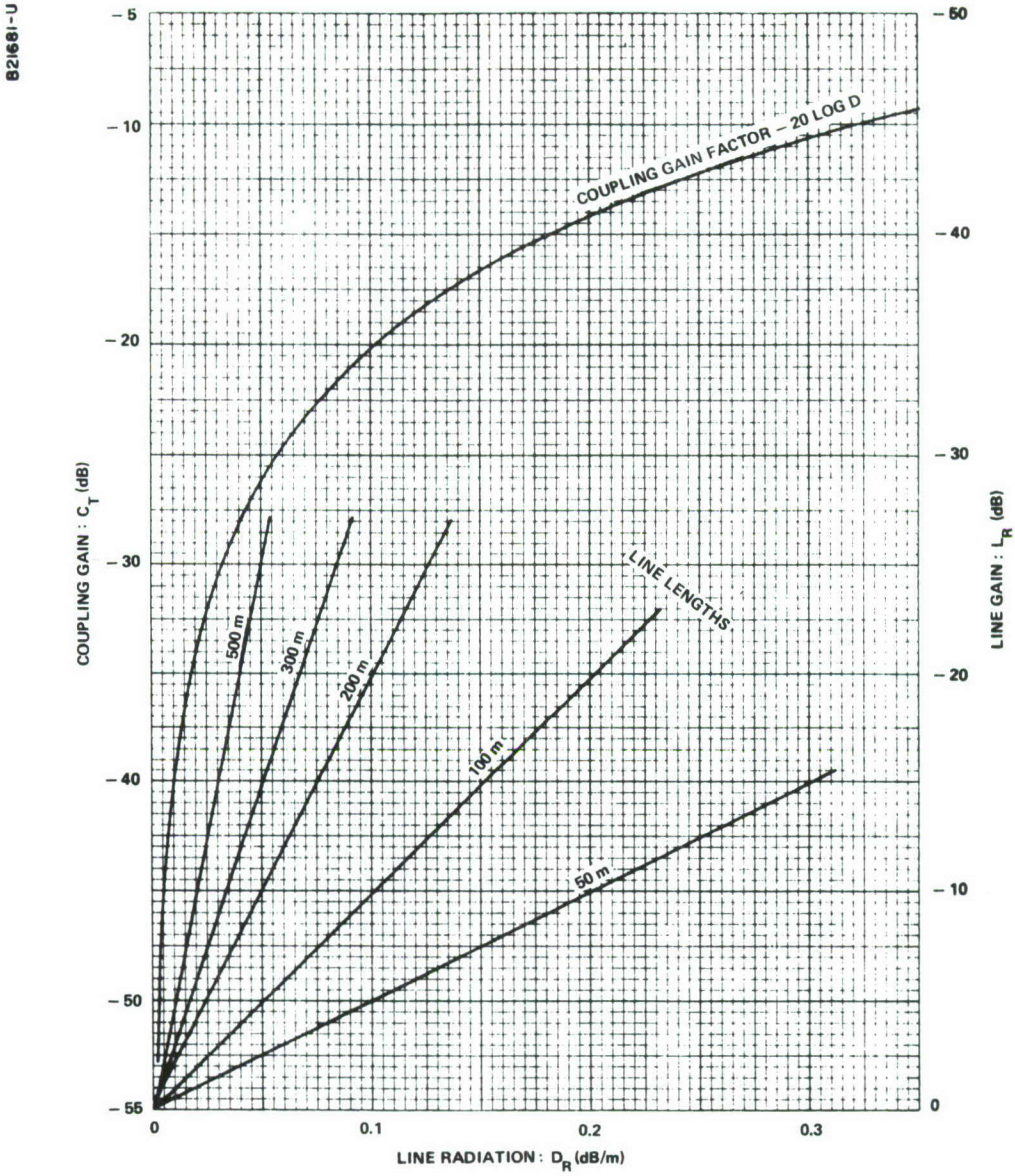

Figure 6 Line Losses and Coupling Factors for Intrusion Detection Line

C_T has been plotted as a function of D_R; S_R for several line lengths (L) has also been plotted as a function of D_R. Optimum performance for any particular line length L will be obtained for the value at which the slope of line plotted for S_R is tangent to the curve for C_T. This is the value of D_R at which small variations in D_R result in equal and opposite changes in S_R and D_T.

The optimum values of D_R have been determined graphically from Figure 6 on this basis and are tabulated in Table 1. The total line radiation loss

OPTIMUM RADIATION LOSS IN DB/METER FOR VARIOUS LINE LENGTHS DETERMINED GRAPHICALLY FROM FIGURE 6.

Line Length Meters	Radiation Loss dB/meter	Total Line Radiation Loss
50	.165	8.2
100	.080	8.0
200	.043	8.6
300	.029	8.7
500	.016	8.0
1000	.008	8.0

Table 1

has also been tabulated, and it will be seen that the optimum performance in all cases requires a total line radiation loss of about 8 dB. Thus as the line becomes longer, the radiation per meter must be reduced to make the total radiation "loss" constant.

The result indicated graphically above can also be obtained analytically and the exact optimum value of D_R can be determined. Referring to Equations (16) and (17), the condition for optimum system sensitivity as a function of D_R corresponds to

$$\frac{d\ S_R}{d\ D_R} = -\frac{d\ C_T}{d\ D_R} \tag{18}$$

and this is found to occur for

$$D_R = \frac{20}{L\ \ln\ 10} = \frac{8.69}{L} \text{ decibels/meter} \tag{19}$$

or,

$$D_R\ L = 8.69 \text{ Decibels} \tag{20}$$

It should be noted that this figure is independent of the dissipative loss factor D_T which is the inherent loss of the line array used. D_T obviously affects the sensitivity of the system, but regardless of what it is, optimum performance occurs for the condition of (19) that $D_R = \frac{8.69}{L}$ decibels/meter. (This supposes that adjustments of D_R do not materially affect D_T which is assumed valid for most situations.)

The values of the various elements of Equation (15) will now be determined for a number of line lengths to show the radar system performance

required. The figures given in the earlier example will be used except for D_R which will be optimized so that L D_R = 8.7 dB. The data previously used are:

r = 3 meters

A = 1 square meter

F = 915 MHz

D_T = 6 dB/100 meters, or .06 dB/meter.

The results are shown in Table 2.

Values for two non-optimum designs are shown for comparison, one of which is the 300 meter line of an earlier example (see Equation (9c)). It will be noted that use of the non-optimum value 30 dB rather than 8.69 dB for L D_R results in a required radar receiver/transmit ratio of -127.6 dB rather than the -117.1 dB performance required for L D_R = 8.69 dB. Thus a 21 dB excess in the value of L D_R increases the radar performance requirement by 10.5 dB. Figure 7 shows numerically the effect of deviation from the optimum value of D_R for several lengths of line.

The required radar performance (transmitter level above receiver signal requirement in dB) for the system of Figure 1 is shown graphically in Figure 8 along with data for normalizing to other conditions. Figure 8 also shows the line radiation factor required in dB/meter for the optimum 8.7 dB radiation for the whole line. The radar performance requirements of Figure 8 are based on L D_R = 8.7 dB.

$$S = -L D_R - L D_T - M + 9.2 + 10 \log \frac{A}{r^2 F^2} + 20 \log D_R$$

L (meters)	S Decibels	$-L D_R$ Decibels	$-L D_T$ Decibels	9.2 Decibels	$10 \log \frac{A}{r^2 F^2}$	$20 \log D_R$	$D_R = \frac{8.7}{L}$ dB/meter
50	- 86.5	- 8.7	- 3	9.2	-68.8	-15.2	.174
100	- 95.5	- 8.7	- 6	9.2	-68.8	-21.2	.087
150	-102.0	- 8.7	- 9	9.2	-68.8	-24.7	.058
200	-107.5	- 8.7	-12	9.2	-68.8	-27.2	.043
300	-117.1	- 8.7	-18	9.2	-68.8	-30.8	.029
500	-133.5	- 8.7	-30	9.2	-68.8	-35.2	.0175
1000	-169.5	- 8.7	-60	9.2	-68.8	-41.2	.0087

Ratio of $\frac{P_r}{P_T}$ for "bistatic" line intrusion detector expressed in decibels for optimum design

46 (150')	- 89.8	-20	- 3*	9.2	-68.8	- 7.2	.435
300	-127.6	-30	-18	9.2	-68.8	-20.0	0.1

*Attentuation D_T = 2 dB/100 feet, or .065 dB/meter

Ratio of $\frac{P_r}{P_T}$ as above but with non-optimum value of D_R

Table 2

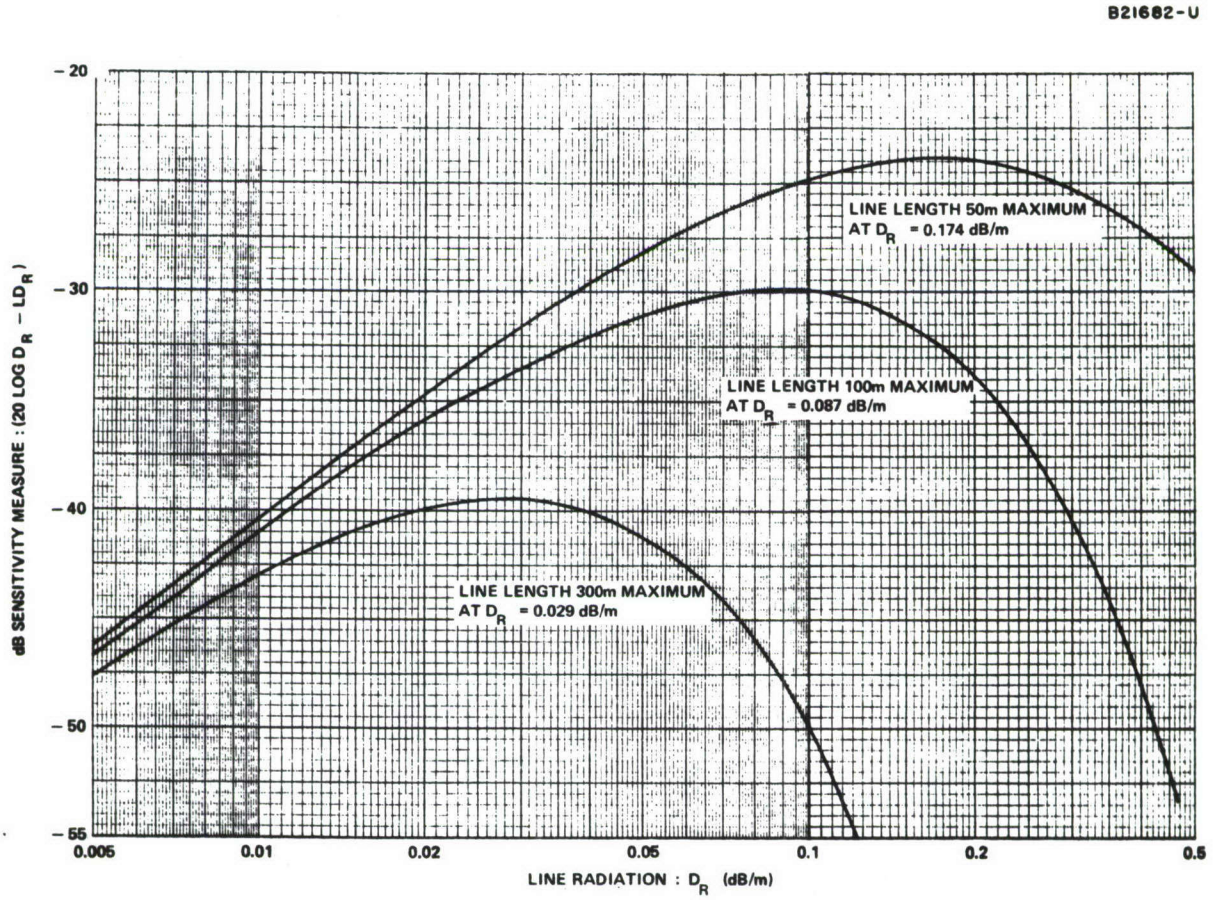

Figure 7 Sensitivity Measure as a Function of Line Radiation in a Bistatic Line Intrusion Detector

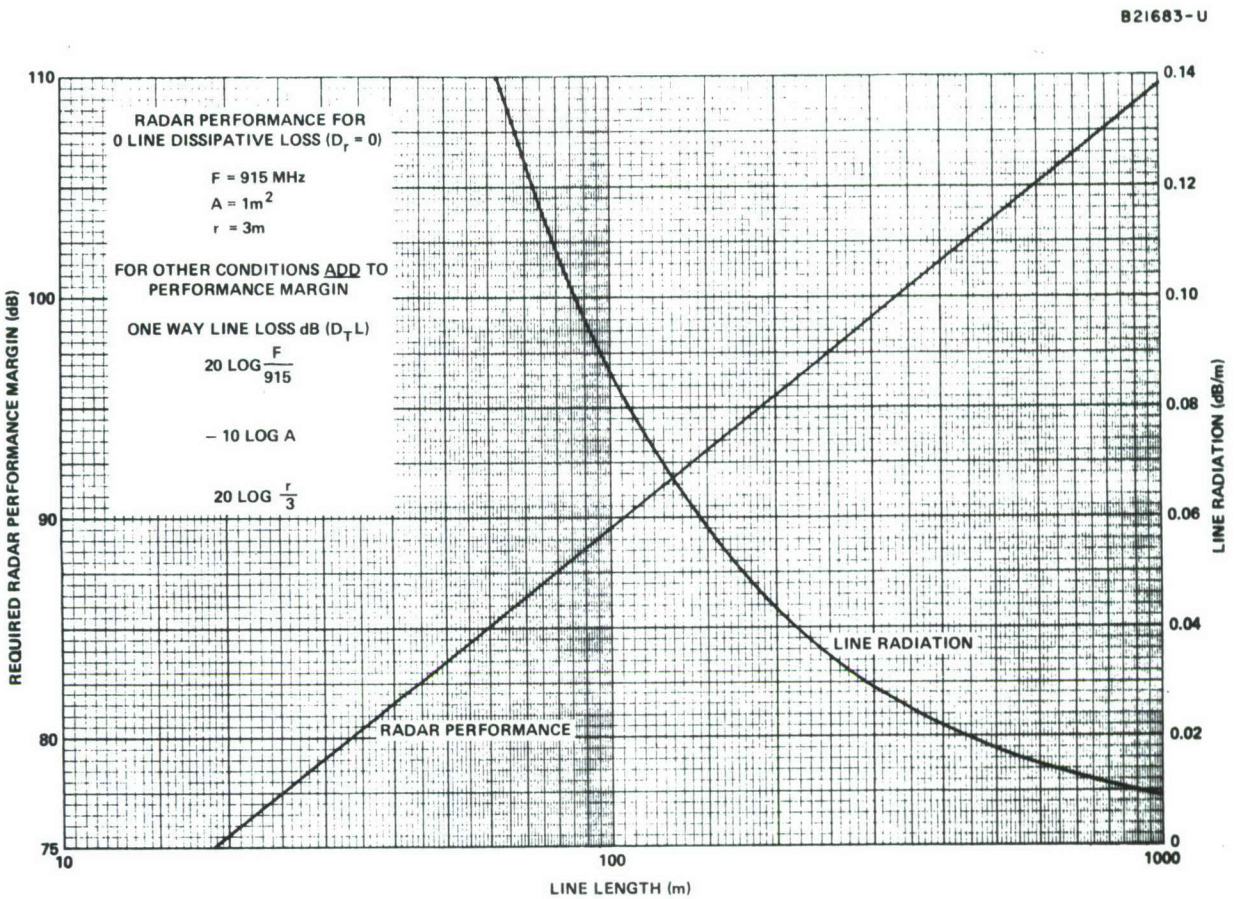

Figure 8 Radar Performance and Line Radiation Required for Bistatic Intrusion Line Radar (Optimum Radiation)

APPENDIX I

Relation of Usual Derivation of Standard Radar Performance to the Method Used for Line Intrusion Radar

Evaluation of the performance of a radar system requires a knowledge of the basic system performance given by the ratio of the signal available at the receiver terminals to that delivered from the transmitter terminals.

The attached pages (Exhibit 1) from a previous paper on Moon Detection Radar gives a derivation of this ratio (see Equation 5-b) in terms of the antenna gain, echoing area, frequency and range for a standard radar system. The same general approach has been used in the derivation of the performance of the line intrusion radar, with one exception.

The line intrusion analysis has introduced the concept of an isotropic antenna scatterer as an elementary target. Such an antenna/scatterer receives such power as it can from the transmitter power flow, and isotropically re-radiates it. Introduction of it allows clear application of the network bilateral nature to logical separation between the path from the transmitter to the target and the path from the target to the receiver. The result is then adjusted to reflect the ratio of the actual effective target area to that of the elementary isotropic antenna.

To support the validity of this concept, Exhibit 2 applies it to the derivation in the Moon Radar paper to show how it can be used in an alternate procedure to go from Equation (1) to Equation (5-b).

It has not been extended to the other equations since the only purpose is to show that it produces a result identical with that obtained by the reasoning originally used in the standard radar formula derivation.

EXHIBIT 1 TO APPENDIX I

Detection of Radio Signals Reflected from the Moon*

JOHN H. DEWITT, JR.†, SENIOR MEMBER, IRE, AND E. K. STODOLA‡, SENIOR MEMBER, IRE

Summary—**This paper describes the experiments at Evans Signal Laboratory which resulted in the obtaining of radio reflections from the moon, and reviews the considerations involved in such transmissions. The character of the moon as a radar target is considered in some detail, followed by development of formulas and curves which show the attenuation between transmitting and receiving antennas in a moon radar system. An experimental radar equipment capable of producing reflections from the moon is briefly described, and results obtained with it are given. Some of the considerations with respect to communication circuits involving the moon are presented. The effects of reflection at the moon on pulse shape and pulse intensity for various transmitted pulse widths are dealt with quantitatively in the Appendix.**

I. Introduction

THE POSSIBILITY of radio signals being reflected from the moon to the earth has been frequently speculated upon by workers in the radio field. Various uses for such reflections exist, particularly in respect to measurement of the refracting and attenuating properties of the earth's atmosphere. Other conceivable uses include communication between points on the earth using the moon as a relaying reflector, and the performance of astronomical measurements.

Late in 1945, a program to determine whether such reflections could be obtained and the uses which might be made of them was undertaken by the U. S. Army Signal Corps at Evans Signal Laboratory, Belmar, N. J. The work has been continued since then, and, although for various reasons progress on it has been slow, this paper has been prepared to indicate the nature of the work and results so far obtained.

II. The Moon as a Radar Target

The moon is approximately spherical in shape, is some 2,160 miles in diameter, and moves in an orbit around the earth at a distance which varies from 221,463 miles to 252,710 miles over a period of about one month.

In considering the type of signals to be used for reflections, the manner in which the reflection occurs must be considered. If it were assumed that the moon were a perfectly smooth sphere, the reflection would be expected to occur from a single small area at the nearest surface, as would be the case with light and a mirror-surfaced sphere. However, astronomical examination of the moon reveals that, in its grosser aspects at least, its terrain consists of plains and mountains of the same magnitude as those on the earth. Further, because of the lack of water and air on the moon to produce weathering, it is probable that the details of the surface are even rougher than the earth. Thus, it is assumed that the type of reflection to be obtained from the moon will resemble the reflections obtained on earth from large land masses, or, to use radar terminology, ground clutter. An example of such a reflection obtained experimentally on earth is shown in Fig. 1. The echoes shown

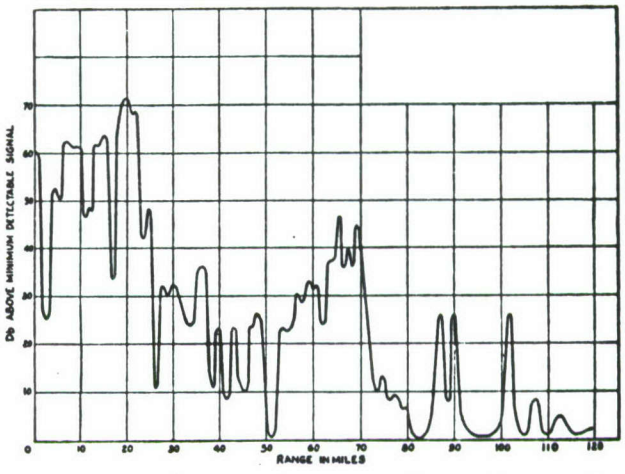

Fig. 1—Reflection obtained from a mountainous region on earth with a 25-microsecond, 106-Mc pulse.

were plotted from observations made with a 25-microsecond 106-Mc pulse transmitted into a mountainous region near Ellenville, N. Y. It will be seen that the intensity of reflection at various ranges varies in a quite random fashion, subject to a general dropping as the range increases. In this case, at 30 miles range and taking the antenna beam width as 12° and for the pulse width of 25 microseconds, or 2.7 miles, the echo at 30 miles range is the averaging of all echoes over an area of about 17 square miles. A pulse of the same width directed at the moon, using equation (35) in the Appendix, may act upon as much as 5,800 square miles. Thus, in the case of the moon, the return echo for a major portion of the time is an averaging of echoes over a very large area and could be expected to exhibit a high degree of constancy per unit projected area.

Thus the most reasonable assumption seems to be that, on the whole, the moon behaves for radio waves much as it behaves for light; that is, when illuminated from the direction of the earth, it presents a disk equal in area to the projected area of the sphere, the disk being illuminated in a generally uniform manner with any bright or dark spots distributed over the disk in a random manner. On the basis of this, it is evident that appreciable power contributions to the returning signal are received from areas on the moon which are at various ranges from the earth. Therefore, if a pulse system is used, to obtain maximum reflection the pulses should be long in time compared to the time required for a radio wave to travel in space the distance from the nearest

* Decimal classification: R537.4. Original manuscript received by the Institute, March 11, 1948.
† Radio Station WSM, Inc., Nashville, Tenn.
‡ Reeves Instrument Corporation, New York, N. Y.

point on the moon to the center and back again, if one is to be certain of the entire half surface of the moon contributing to the reflection. Since this distance is two times 2,160/2 miles and the velocity of propagation is about 186,000 miles per second, this time interval is 2,160/186,000 = 0.0116 second.

Thus, provided the pulse used for tests is appreciably greater than 0.0116 second, the moon is assumed to act as an isotropic reflector which has an area equal to the projected area of the sphere. Thus, for a wide pulse, the reflecting area of the moon is $\pi r^2 = \pi(2{,}160/2)^2 = 3.66 \times 10^6$ square miles, or 9.48×10^{12} square meters.

However, since the moon's surface is not a perfect conductor, this area must be multiplied by a reflection coefficient to account for the fact that all of the energy impinging is not reflected. With a target of this type, which assumes that the projected disk of the moon acts as a uniform reflector, the reflection coefficient for normal incidence would seem to be appropriate. A value of 17 per cent is given for the reflection coefficient of earth by Stratton.[1]

In the above discussion no attention has been given to the effect of depolarization of the wave by the reflection at the moon. This will probably cause some further reduction in effective reflection coefficient of the moon, but such further reduction is assumed to be not significantly large.

In the Appendix, the quantitative implications of this concept are considered, and it is shown that any pulse signal impinging on the moon is broadened by 0.0116 second. For pulses less than 0.0116 second duration, the maximum area effective in creating a reflection depends upon the pulse width, according to a curve given in Fig. 18 of the Appendix, so that, for a 1-microsecond pulse, the maximum effective area is only 0.00017 of the full disk area, representing a decrease in available peak signal of 37.7 db.

The previous discussion is primarily concerned with the case in which the antenna beam illuminates the entire disk of the moon in a uniform manner. If the beam is narrow enough to illuminate only a portion of the moon, the same type of considerations also apply, but spreading of pulses because of the bulk of the moon is reduced.

III. Attenuation in the Earth-Moon-Earth Path

The ratio of the signal power available at the receiver terminals to that available from the transmitter is a factor which must be known to determine the type of equipment capable of performing the experiment. This ratio may be determined in the following manner:[2,3]

At a range R from the transmitting antenna the power flow S_0 per unit area is

$$S_0 = \frac{P_t G_t}{4\pi R^2} \tag{1}$$

where

P_t = transmitter power

G_t = transmitter antenna gain over isotropic radiator

R = range.

This power impinges on the equivalent isotropic echoing area of the target A_E, is attenuated by the reflection coefficient m of the target,[4] is then re-radiated and is subject to the same spherical dispersion, so that the power flow at the receiving point S_R is given by

$$S_R = \frac{S_0 A_E m}{4\pi R^2} = \frac{P_t G_t A_E m}{16\pi^2 R^4}. \tag{2}$$

This power flow impinges on the receiving antenna of area A_R to give an available received power of

$$P_R = S_R A_R = \frac{P_t G_t A_E A_R m}{16\pi^2 R^4}. \tag{3}$$

The relation of gain to effective antenna area is given by

$$A_R = \frac{G_R \lambda^2}{4\pi} \text{ (square meters)} \tag{4a}$$

where λ is the wavelength in meters, or, since $\lambda = 300/F$, where F is the radio frequency in megacycles, and

$$A_R = \frac{7160 G_R}{F^2} \text{ (square meters)}. \tag{4b}$$

Substituting (4a) or (4b) in (3) and noting that $G_T = G_R = G$ for radar-type operations, and that because of the units of (4a) and (4b) all distances must be in meters,

$$\frac{P_R}{P_t} = \frac{G^2 A_E \lambda^2 m}{1984 R^4} \tag{5a}$$

or

$$\frac{P_R}{P_t} = \frac{45.4 G^2 A_E m}{F^2 R^4}. \tag{5b}$$

It is also of interest to have the formulas in terms of the receiving and transmitting antenna area A_R. These can be obtained by combining (3) and (4a) or (4b), again taking $G_R = G_t$ to give

$$\frac{P_R}{P_t} = \frac{A_R^2 A_E m}{4\pi \lambda^2 R^4} \tag{6a}$$

or

$$\frac{P_R}{P_t} = \frac{A_R^2 A_E F^2 m}{1.13 \times 10^6 R^4}. \tag{6b}$$

SEE EXHIBIT 2 FOR ALTERNATE METHOD FOR THIS TRANSITION

[1] J. A. Stratton, "Electro-Magnetic Theory," McGraw-Hill Book Co., New York, N. Y., First Edition, p. 510; 1941.

[2] K. A. Norton and A. C. Omberg, "Maximum range of a radar set," report ORG-P-9-1 issued by the Chief Signal Officer, War Department, Washington, D. C. February, 1943; and Proc. I.R.E., vol. 35, pp. 4–24; January, 1947.

[3] The treatment is given sketchily here, as it follows generally the method of the reference.

[4] The effect of area of the target and its reflection coefficient m are kept separate in this treatment to avoid later confusion.

The formulas (5) and (6) are based on the tacit assumption that the beam width of the antenna is sufficiently large that the moon is illuminated over its entire surface by the transmitted beam. If the beam width is so narrow that the entire beam falls on the moon, then the moon can be considered as an isotropic source radiating the transmitter power reduced by the reflection coefficient m, and the power received back at the earth is simply

$$P_R = \frac{P_t A_R m}{4\pi R^2}, \tag{7a}$$

whence

$$\frac{P_R}{P_t} = \frac{A_R m}{4\pi R^2}, \tag{7b}$$

and substituting the values of (4a) and (4b) in (7b) gives

$$\frac{P_R}{P_t} = \frac{G_R \lambda^2 m}{16\pi^2 R^2} \tag{8a}$$

or

$$\frac{P_R}{P_t} = \frac{570 G_R m}{F^2 R^2}. \tag{8b}$$

Equations (5) and (6) hold for relatively wide beam widths, while (7) and (8) hold for very narrow beam widths. Since antennas do not have sharply defined beams of uniform density, the transition from the region where (5) and (6) are valid to the region where (7) and (8) are valid is not a sudden one, and neither one is precise in the region of transition. However, the region in which the transition occurs can be determined by assuming that the values of P_R/P_T obtained from each equation are equal and calculating the relations which must exist for their equality. Equating (6a) and (7b) gives

$$\frac{A_R^2 A_R m}{4\pi\lambda^2 R^4} = \frac{A_R m}{4\pi R^2},$$

and writing the area of the moon's disk at πr^2 where r is the radius of the moon, and the area of the antenna A_R as $\pi D'^2/4$ where D' is the diameter of the antenna aperture in meters, gives

$$\frac{r}{R} = \frac{\lambda}{D'} \cdot \frac{2}{\pi}. \tag{9}$$

Now, if α = the angle subtended by the moon, and since α is a very small angle, $\alpha/2 = r/R$, substituting in (9) and solving for α gives

$$\alpha = 1.28 \frac{\lambda}{D'} \tag{10}$$

where α is expressed in radians.

From the earth, the moon subtends an angle of almost exactly 1/2° or 0.0087 radians, the precise amount depending upon the exact position of the moon in its orbit. At its most distant point (apogee), this angle is 2,160/252,710 = 0.00855 radian. If such value be placed in (10), then $\lambda/D' = 0.00855/1.28$ gives the value of λ/D' at which the transition of validity from (5) and (6) to (7) and (8) occurs. Converting to a more useful form, the substitution of $\lambda = 300/F$ where F is the frequency in megacycles, and $D' = D/3.28$ where D is in feet (D' in meters), is made. Using these, it may then be said that (7) and (8) should be used for

$$FD > 1.46 \times 10^5, \quad \text{or} \quad F > \frac{146 \times 10^3}{D} \tag{11}$$

where F is in megacycles and D is in feet.

In the case of a square-aperture antenna, the same general considerations approximately apply, if D is taken as the length of one side.

In order to determine the actual attenuation involved, it is necessary to insert in (6b) the values for R and A_R. R will be taken as the maximum range, 252,710 miles or 4.07×10^8 meters. The area has previously been given as 9.48×10^{13} square meters, and the reflection coefficient m as 0.17. The area in square meters of a round-aperture antenna is $\pi D^2/4 \times 10.75$ where D is in feet. Substituting these values in (6b) gives

$$\frac{P_R}{P_t} = 2.77 \times 10^{-31} D^4 F^2 \tag{12}$$

where D is the effective antenna diameter in feet and F is in megacycles. Performing a similar substitution in (7b), one obtains

$$\frac{P_R}{P_t} = 5.97 \times 10^{-21} D^2 \tag{13}$$

where D is the effective antenna diameter in feet.

In practical antennas it is usually not possible to obtain the gain given by (4) because the aperture is usually not uniformly illuminated, either because of practical difficulties or to reduce side lobes in the pattern. The effective diameter of a round-aperture antenna should be taken as about 85 per cent of its physical diameter in applying (11), (12), and (13), so that, for practical antennas, (12), (11), and (13), respectively, become

$$\frac{P_R}{P_t} = 1.448 \times 10^{-31} D^4 F^2. \tag{14}$$

The above is true for low frequencies. If

$$F \geq \frac{172 \times 10^3}{D}, \tag{15}$$

then

$$\frac{P_R}{P_t} = 4.31 \times 10^{-21} D^2 \tag{16}$$

where, in each case, D is the actual antenna-aperture diameter in feet and F is the radio frequency in megacycles.

The results of these equations are shown in Fig. 2. The solid curves give the attenuation for various sizes of antenna apertures, as indicated. The dashed line indicates the transition between a beam wider than the moon and one narrower. As indicated previously, this transition does not occur abruptly as in these idealized curves, but the curves do give a basis for close estimation of the system requirement.

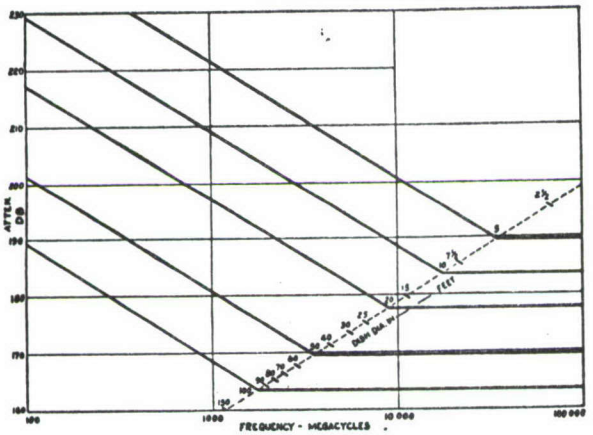

Fig. 2—Attenuation of the earth-moon-earth radar path for various frequencies and antenna apertures.

In all of the above, no effects of attenuation due to losses in the atmosphere or space, nor to the effect of refraction in the atmosphere, have been considered. However, at frequencies in the range from 100 to perhaps a few thousand megacycles, it is probable that for a considerable portion of the time these effects will not materially affect the attenuation figures given in the curve, since shorter-range radar operation in this frequency range gives results which are consistent with the assumption of negligible losses in the atmosphere and, with some exceptions, no refraction effects.

At frequencies much below 100 Mc, ionospheric refraction or reflection effects become much more pronounced, and it is probable that signals could not be sent to the moon and back at these lower frequencies.

It should also be noted that, in the above discussion, no attention has been given to ground reflections. If the antenna beam width is wide enough and the angle at which the antenna is aimed is low enough so that the ground is heavily illuminated by the beam, the ground-reflected wave will, at certain elevation angles, reinforce the direct wave, so that, under ideal conditions, the antenna gain will be increased by 6 db, and the over-all attenuation of Fig. 2 may be reduced under these conditions by as much as 12 db.

Equipment Requirements

The attenuations shown in Fig. 2 for ordinarily used antenna sizes are considerably in excess of the spread between transmitter power and minimum detectable signal for the receiver in a usual radar system. Further, as shown in the Appendix, to obtain attenuation even as small as shown in Fig. 2, a pulse width in excess of 12,000 microseconds is necessary, so that consideration of ordinary radar systems is ruled out on this ground, in addition to the long travel time to the moon and back which makes desirable the use of a low pulse-repetition rate.

Fig. 3 gives a basis on which the performance of a radar system may be approximately estimated. The input noise power with which a signal must compete is given by $P_{noise} = KTB$ where K = Boltzmann's constant $= 1.37 \times 10^{-23}$ joules/degree, T is the effective input (antenna) resistance temperature in °K, and B is the bandwidth in cps. This figure must in increased by the noise factor of the receiver.[5,6-7]

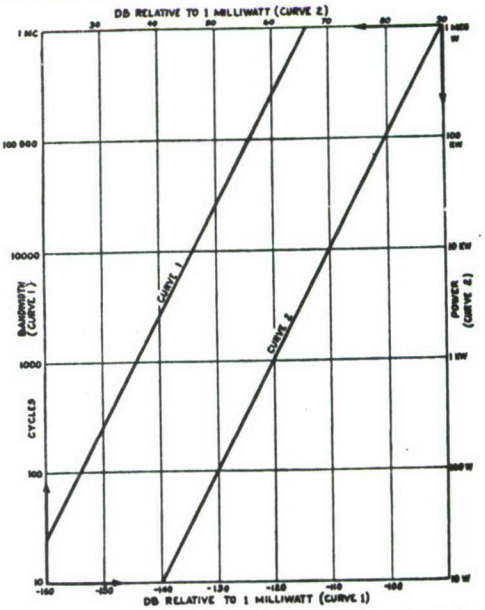

Fig. 3—Johnson noise and transmitter power levels in decibels with respect to 1 milliwatt.

If the pulse width of a radar transmitter is approximately (by a factor of from 1/2 to 2) equal in seconds to the reciprocal of receiver intermediate-frequency-amplifier bandwidth in cps, the minimum detectable signal will be of the order of the effective input noise (that is, KTB increased by the noise factor). It can be assumed that the effective antenna resistance is at a temperature of 300°K and, even if this assumption is not precise, when the noise factor referred to this temperature is not too close to 1, the error introduced by a lower effective antenna temperature will not be serious. The minimum detectable signal is also affected by pulse-repetition rate and other factors, but the above consideration gives a useful initial approximation.

[5] The references given are relevant to this and later discussion.
[6] A. V. Haeff, "Minimum detectable radar signal and its dependence upon the parameters of radar systems," Proc. I.R.E., vol. 34, pp. 857–861; November, 1946.
[7] H. T. Friis, "Noise figures of radio receivers," Proc. I.R.E., vol. 32, pp. 419–422; July, 1944.

EXHIBIT 2 to APPENDIX I

Alternate Method of Proceeding from Equation (1) to Equation (5b) Of DeWitt/Stodola Paper Using Concept of an Isotropic Antenna as The Elementary Target-Scatterer

PROCEEDINGS OF THE I.R.E. *March* (1949)

At a range R from the transmitting antenna the power flow S_0 per unit area is

$$S_0 = \frac{P_t G_t}{4\pi R^2} \qquad (1)$$

where
P_t = transmitter power
G_t = transmitter antenna gain over isotropic radiator
R = range.

Consider as an elementary scatterer an isotropic antenna which absorbs power from the direction of arrival and then reradiates it isotropically.

The effective area of an antenna is related to its gain by

$$A = \frac{7160\ G}{F^2} \qquad \text{(Corresponds to 4b in paper)} \qquad (1a)$$

The effective area of an isotropic antenna (G=1) is A_T;

$$A_T = \frac{7160}{F^2}$$

At the range R this will capture $S_o A_T = P_a$ watts. so. combining with (1),

$$P_a = P_T \left(\frac{G_t\ 7160}{4\pi R^2\ F^2} \right) \qquad (1b)$$

Since the network from transmitter antenna terminals to the target antenna terminals is a bilateral one, the attenuation suffered by P_T in going from the transmit antenna terminals to the isotropic antenna-scatterer terminals $\left(\frac{P_a}{P_T}\right)$ will also be suffered by the power P_a reradiated from the isotropic antenna in returning to the transmitter antenna terminals which are also the receiving antenna terminals since use of the same antenna of gain G for both purposes is assumed. Thus,

$$\frac{P_a}{P_t} = \frac{P_R}{P_a} = \frac{G\ 7160}{4\pi\ R^2\ F^2} \tag{1c}$$

where P_R = available received power at the radar antenna terminals.

$$\frac{P_R}{P_t} = \frac{P_a}{P_t} \times \frac{P_R}{P_a} = \left(\frac{G\ 7160}{4\pi\ R^2\ F^2}\right)^2 = \frac{(7160)^2\ G^2}{16\pi^2\ R^4\ F^4} \tag{1d}$$

The actual target used in general has an area different from that of the isotropic antenna-scatterer, $\frac{7160}{F^2}$.
Hence the value of $\frac{P_R}{P_t}$ actually obtained with a scatterer having an actual effective echoing area of A_E^m will be that of Equation (1d) multiplied by the area ratio which is $A_E^m/\frac{7160}{F^2}$. Multiplying (1d) by the quantity gives

$$\frac{P_R}{P_t} = \frac{7160\ G^2\ A_E^m}{16\pi^2\ R^4\ F^2} \quad ,$$

or

$$\frac{P_R}{P_t} = \frac{45.4 G^2 A_E m}{F^2 R^4} . \tag{5b}$$

It is also of interest to have the formulas in terms of the receiving and transmitting antenna area A_R. These can be obtained by combining (3) and (4a) or (4b), again taking $G_R = G_t$ to give

$$\frac{P_R}{P_t} = \frac{A_R^2 A_E m}{4\pi\lambda^2 R^4} \tag{6a}$$

or

$$\frac{P_R}{P_t} = \frac{A_R^2 A_E F^2 m}{1.13 \times 10^4 R^4} . \tag{6b}$$

[4] The effect of area of the target and its reflection coefficient m are kept separate in this treatment to avoid later confusion.

APPENDIX 2

EXAMPLE OF RESISTIVE ATTENUATING NETWORK
TO SHOW BILATERAL PROPERTIES

(Calculations Simplified by Neglecting Loading
Effect on Low Value Resistances by High Value
Parallel Resistances)

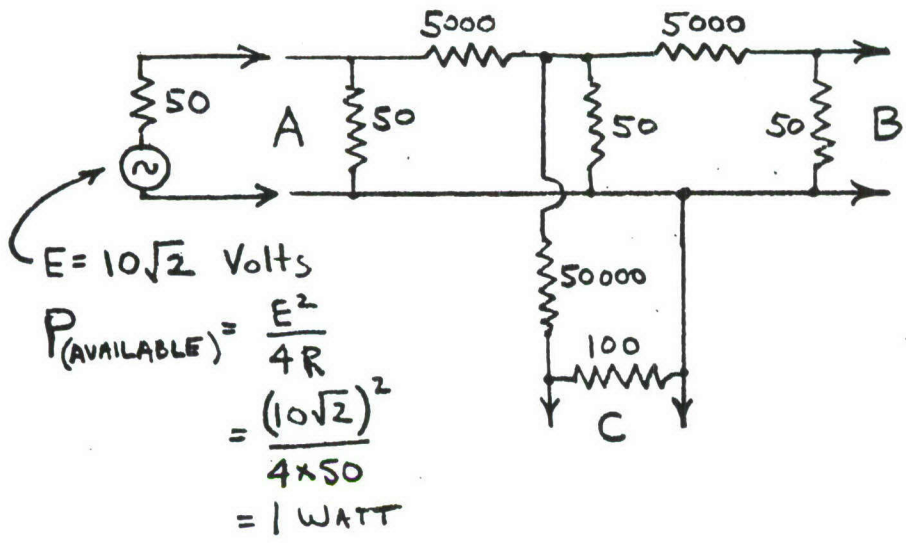

A generator of 1 watt available power is applied at port A of the above network and the available power determined at ports B and C to evaluate the attenuation.

$$E_{B(\text{open circuit})} = 10\sqrt{2} \times \frac{1}{2} \times \frac{50}{5000} \times \frac{50}{5000} = \frac{1}{\sqrt{2}} \times 10^{-3} \text{ volts}$$

$$P_{B(\text{Available})} = \frac{E^2}{4R} = \left(\frac{1}{\sqrt{2}} \times 10^{-3}\right)^2 / 4 \times 50 = 2.5 \times 10^{-9} \text{ watts}$$

$$\text{Power Ratio}_{(B \text{ to } A)} = 2.5 \times 10^{-9}, \text{ or, } -86 \text{ dB} \qquad (1)$$

$$E_{c(\text{Open circuit})} = 10\sqrt{2} \times \frac{1}{2} \times \frac{50}{5000} \times \frac{100}{50000} = \sqrt{2} \times 10^{-4} \text{ volts}$$

$$P_{c(\text{Available})} = \frac{E^2}{4R} = \frac{\left(\sqrt{2} \times 10^{-4}\right)^2}{4 \times 100} = 5 \times 10^{-11} \text{ watts}$$

$$\text{Power Ratio}_{(\text{C to A})} = 5 \times 10^{-11}, \text{ or } -103 \text{ dB} \qquad (2)$$

Now consider a 1 watt available power generator applied at C, and determine the powers available at A and B.

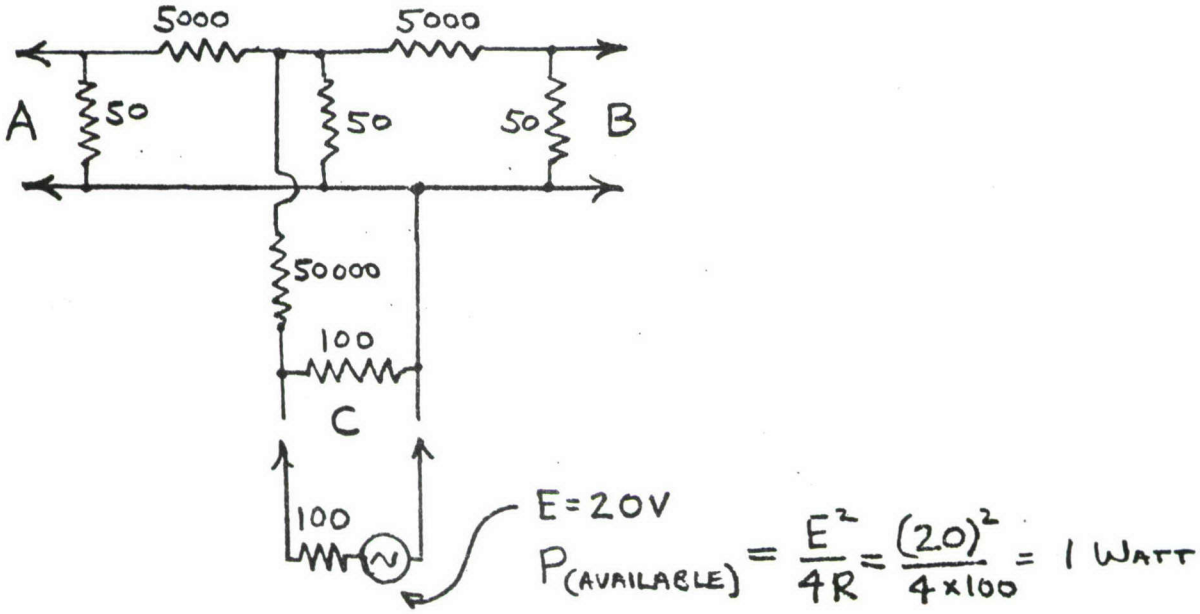

$$E_{A(\text{open circuit})} = 20 \times \frac{1}{2} \times \frac{50}{50000} \times \frac{50}{5000} = 10^{-4} \text{ volts}$$

$$P_{A(\text{Available})} = \frac{E^2}{4R} = \frac{\left(10^{-4}\right)^2}{4 \times 50} = 5 \times 10^{-11} \text{ watts}$$

$$\text{Power Ratio}_{(\text{A to C})} = 5 \times 10^{-11}, \text{ or } -103 \text{ dB} \qquad (3)$$

Thus it will be seen that the power ratio (2) from A to C is - 103 dB and the ratio from C to A is also - 103 dB, verifying the bilateral nature of the network. Note that the available power ratios must be considered rather than just voltage or current ratios. It should also be noted that the ratio of P_B to P_C will be the same as the ratio (3) of P_A to P_C, since the C-A and C-B paths are symmetrical and the same voltage divisions will occur.

DISTRIBUTION LIST

	Copies
Commander US Army Materiel Command ATTN: AMCDL 5001 Eisenhower Avenue Alexandria, VA 22333	1
Commander US Army Materiel Command ATTN: AMCRD 5001 Eisenhower Avenue Alexandria, VA 22333	3
Commander US Army Materiel Command ATTN: AMCRD-P 5001 Eisenhower Avenue Alexandria, VA 22333	1
Director of Defense, Research & Engineering Department of Defense WASH DC 20301	1
Director Defense Advanced Research Projects Agency WASH DC 20301	3
HQDA (DARD-DDC) WASH DC 20310	4
HQDA (DARD-ARZ-C) WASH DC 20310	1
HQDA (DAFD-ZB) WASH DC 20310	1
HQDA (DAMO-PLW) WASH DC 20310	1
Commander US Army Training & Doctrine Command ATTN: ATCD Fort Monroe, VA 23651	1

Commander 1
US Army Combined Arms Combat Developments Activity (PROV)
Fort Leavenworth, KS 66027

Commander 1
US Army Logistics Center
Fort Lee, VA 23801

Commander 1
US Army CDC Intelligence & Control Systems Group
Fort Belvoir, VA 22060

TRADOC Liaison Office 1
HQS USATECOM
Aberdeen Proving Ground, MD 21005

Commander 1
US Army Test and Evaluation Command
Aberdeen Proving Ground, MD 21005

Commander 1
US Army John F. Kennedy Center for Military Assistance
Fort Bragg, NC 28307

Commander-In-Chief 1
US Army Pacific
ATTN: GPOP-FD
APO San Francisco 96558

Commander 1
Eighth US Army
ATTN: EAGO-P
APO San Francisco 96301

Commander 1
Eighth US Army
ATTN: EAGO-FD
APO San Francisco 96301

Commander-In-Chief 4
US Army Europe
ATTN: AEAGC-ND
APO New York 09403

Commander 1
US Army Alaska
ATTN: ARACD
APO Seattle 98749

Commander 1
MASSTER
ATTN: Combat Service Support & Special Programs Directorate
Fort Hood, TX 76544

Commander 2
US MAC-T & JUSMAG-T
ATTN: MACTRD
APO San Francisco 96346

Senior Standardization Representative 1
US Army Standardization Group, Australia
c/o American Embassy
APO San Francisco 96404

Senior Standardization Representative 1
US Army Standardization Group, UK
Box 65
FPO New York 09510

Senior Standardization Representative 1
US Army Standardization Group, Canada
Canadian Forces Headquarters
Ottawa, Canada K1A0K2

Director 1
Air University Library
ATTN: AUL3T-64-572
Maxwell Air Force Base, AL 36112

Battelle Memorial Institute 1
Tactical Technical Center
Columbus Laboratories
505 King Avenue
Columbus, OH 43201

Defense Documentation Center (ASTIA) 12
Cameron Station
Alexandria, VA 22314

Commander 2
Aberdeen Proving Ground
ATTN: STEAP-TL
Aberdeen Proving Ground, MD 21005

Commander 1
US Army Edgewood Arsenal
ATTN: SMUEA-TS-L
Aberdeen Proving Ground, MD 21010

US Marine Corps Liaison Officer
Aberdeen Proving Ground, MD 21005 — 1

Director
Night Vision Laboratory
US Army Electronics Command
ATTN: AMSEL-NV-D (Mr. Goldberg)
Fort Belvoir, VA 22060 — 1

Commander
US Air Force Special Communications Center (USAFSS)
ATTN: SUR
San Antonio, TX 78243 — 1

Commander
US Army Armament Command
ATTN: AMSAR-ASF
Rock Island, IL 61201 — 1

Mr. E. King Stodola
7816 Heritage Circle
Manlius, NY 13104 — 1

Mr. William Emeny
Mr. Jack Monson
Syracuse University Research Corp.
Merrill Lane, University Heights
Syracuse, NY 13210 — 2

Mr. William York
Aerospace Research Inc.
130 Lincoln Street
Boston, MA 02135 — 1

Mr. Robert Brubaker
CM/CI Dept.
MERDC
Ft. Belvoir, VA 22060 — 1